

Utah State University

DigitalCommons@USU

---

All Graduate Plan B and other Reports

Graduate Studies

---

8-2011

## Modeling Phloem Temperatures Relative to Mountain Pine Beetle Phenology

Matthew Jared Lewis  
*Utah State University*

Follow this and additional works at: <https://digitalcommons.usu.edu/gradreports>



Part of the [Applied Mathematics Commons](#), and the [Mathematics Commons](#)

---

### Recommended Citation

Lewis, Matthew Jared, "Modeling Phloem Temperatures Relative to Mountain Pine Beetle Phenology" (2011). *All Graduate Plan B and other Reports*. 60.  
<https://digitalcommons.usu.edu/gradreports/60>

This Report is brought to you for free and open access by the Graduate Studies at DigitalCommons@USU. It has been accepted for inclusion in All Graduate Plan B and other Reports by an authorized administrator of DigitalCommons@USU. For more information, please contact [digitalcommons@usu.edu](mailto:digitalcommons@usu.edu).



# MODELING PHLOEM TEMPERATURES RELATIVE TO MOUNTAIN PINE BEETLE DEVELOPMENT

by

Matthew Lewis

A report submitted in partial fulfillment  
of the requirements for the degree

of

MASTER OF SCIENCE

in

Mathematics

Approved:

---

Dr. James Powell  
Major Professor

---

Dr. Barbara Bentz  
Committee Member

---

Dr. Richard Cutler  
for Dr. Zhi Qiang Wang  
Committee Member

UTAH STATE UNIVERSITY  
Logan, Utah

2011

# Modeling phloem temperatures relative to mountain pine beetle phenology

Matthew Lewis<sup>1</sup>

Department of Mathematics

Utah State University

Logan, UT 84321

matthew.lewis@aggiemail.usu.edu

August 23, 2011

## Abstract

We explore a variety of methods to estimate phloem temperatures from ambient air temperatures suitable for the mountain pine beetle, *Dendroctonus ponderosae*. A model's ability to induce the same phenology generated from observed phloem temperatures measures its effectiveness rather than a simple reconstruction of phloem temperatures. From a model's phenology results we are able to ascertain whether the model produces a similar amount of developmental energy exhibited by observed phloem temperatures.

Three models performed best: Newton, Newton South and Matching. The Newton model uses Newton's Law of Cooling to effectively estimate northern aspect phloem temperatures. The Newton South model also employs Newton's Law of Cooling but has an additional error parameter used to predict southern aspect phloem temperatures. The Matching model uses a "reverse boot-strapping" method that matches ambient extremes to an archive of air and corresponding phloem temperatures. The archived phloem temperatures that fit best, based on how closely the air extrema match, are successfully used as predicted temperatures. Phenology generated from these models is shown to effectively mimic the phenology produced from observed phloem temperatures in a variety of geographically distinct areas.

---

<sup>1</sup>A project report for Utah State University MS Mathematics Degree

# 1 Introduction

The mountain pine beetle (MPB), *Dendroctonus ponderosae* is a devastating, natural predator of pine trees. While MPB populations occasionally erupt into massive outbreaks that can destroy thousands of hectares, typically, MPB populations remain relatively small, successfully attacking stressed or damaged trees. However, MPB can kill up to 70 to 90 percent of lodgepole pines in many stands while affecting recreational value, altering water production during runoff and limiting access to wildlife and domestic livestock (Safranyik et al., 1974; Amman and Schmitz, 1988; McGregor and Cole, 1985).

Some pine species, such as the lodgepole pine, *Pinus contorta*, have developed a normative relationship with the MPB. Since Lodgepole pines grow best in direct sun, they are able to take advantage of areas denuded by MPB attack. On the other hand, other suitable species, such as high-elevation five-needle pines (e.g. bristlecone, *Pinus aristata*, *Pinus longaeva*; limber, *Pinus flexilis*; whitebark, *Pinus albicaulis*) (Amman, 1982; Means, 2011) have become increasingly more vulnerable to MPB attack. Many of these species are critical to their local ecologies, benefiting wildlife while maintaining and distributing snow pack which in turn provides spring moisture and impacts human populations at lower elevations. These sensitive pine species are historically protected from the ravages of the MPB by the harshness of the environments in which they grow. At the higher elevations, the MPB does not typically receive sufficient solar input in order to sustain univoltinism (one brood per year), which has been linked to MPB success (Logan and Bentz, 1999). Yet, it has been observed and is predicted that, due to climate change, MPB populations can be successful in higher elevation pine stands (Hicke et al., 2006; Logan and Powell, 2001; Carroll et al., 2004; Logan et al., 2003; Bentz et al., 2010). As MPB populations in high elevations become increasingly successful, MPB attacks can directly affect the distribution of water as well as impacting that region's wildlife (Mattson and Jonkel, 1990).

Since MPB are economically and ecologically significant insects there is great interest in modeling their development. Different aspects of MPB phenology can be described based on temperature dependent developmental rate curves that vary depending on MPB life-stage; these rate curves are described more fully in Jenkins et al. (2001). However, the developmental environment of the MPB is not the open air; it is the phloem, or inner-bark, of the bole. Hence, it is the phloem

temperatures that drive MPB development (Powell and Logan, 2005; Powell and Bentz, 2009).

Since phloem temperatures are the driving force in MPB development, there is an effort underway to collect phloem temperatures in a variety of locations. In order to collect phloem temperatures, temperature probes are placed in the phloem 1.8m above the ground on both the north and south side. Phloem temperatures are then measured every 15 minutes, averaged, and recorded each hour as northern and southern aspect hourly phloem temperatures. At the same time, the corresponding ambient air temperatures are recorded using a shielded temperature probe about 1.8m above the ground (Bentz and Mullins, 1999).

Once phloem temperatures are collected, MPB rate curves can then be applied. This results in phloem temperature propelled MPB developmental rate curves that properly describe the developmental energy driving MPB phenology. MPB phenology models have been developed using these rate curves so that, given a certain number of phloem temperatures, one can predict MPB population growth rates (R-function, Powell and Bentz (2009)), number of generations per year (MPB Voltinism, Powell and Logan (2005)), the timing of a population's emergence (Extended von Foerster, Gilbert et al. (2004)) and the stabilizing dynamics of a population (G-function, Powell and Logan (2005)) among others. So, with phloem temperatures and the use of mathematical models we can describe, in broad strokes, many of the prominent aspects of MPB developmental timing.

Since the MPB phenology models are ideally driven by phloem temperatures, phloem temperatures have been collected in a variety of locales; we focus on three: the Stanley valley, Railroad Ridge and the Dixie National Forest. The Stanley valley of the Sawtooth National Recreation Area (SNRA) in central Idaho is an area that is within the MPB's historic geographic domain, where the MPB have been studied for an extended length of time. These studies have produced a large phloem temperature record that has been collected from lodgepole pines, the area's dominant host, along with the corresponding ambient temperatures. Furthermore, MPB phenology models were developed using data collected in the SNRA (Logan and Bentz, 1999; Logan and Powell, 2001; Powell and Logan, 2005; Powell and Bentz, 2009). For a fuller description of the SNRA see Powell and Bentz (2009).

Similar to the Stanley valley, the Dixie National Forest (DNF), located in southern Utah is also an area within the MPB's typical domain. There are however key differences between the DNF

and the SNRA that make the DNF an attractive location. Firstly, the temperatures in southern Utah tend to be much warmer than the temperatures in central Idaho. Secondly, the dominant host MPB host species in the DNF is the ponderosa pine, *Pinus ponderosa*. Details of collection of phloem temperatures and geography of the DNF and SNRA sites appear in Bentz and Mullins (1999).

Railroad Ridge (RRR), located in central Idaho in the White Cloud Mountains also differs from both the SNRA and DNF in climate and dominant host species. RRR, is at an elevation around 3000 m, much cooler than both the SNRA and DNF. The dominant host species is whitebark pine, an important and fragile high-elevation five-needle pine. Railroad Ridge is more fully described in Logan and Powell (2001).

Even with phloem temperatures from a variety of locations, it is still difficult to predict MPB phenology. One difficulty is choosing which phloem temperatures to use since they can vary from tree to tree and also within the tree (figure 1). This difference in temperatures has been attributed to solar insolation as well as re-radiation from the surrounding environment (Powell and Bentz, 2009). While the north-side tree bole temperatures “look” similar to the ambient temperatures, some of the MPB phenology models generate more accurate predictions when phloem temperatures collected from the southern aspect of the bole are used (Powell and Bentz, 2009). As is evident from figure 1, southern aspect phloem temperatures can vary greatly from ambient temperatures. Furthermore, ambient temperatures can be a poor substitute for phloem temperatures Powell and Bentz (2009).

While the USDA Forest Service’s Rocky Mountain Research Station Forestry Sciences Laboratory in Logan, UT has been expanding the range of phloem temperature measurements, there are still relatively few areas where phloem temperatures have been consistently measured, there is a wealth of measured ambient air temperatures. To use the existing MPB phenology models in more areas, a connection must be made between ambient air temperatures and phloem temperatures. This is especially critical as climatic warming trends have coincided with massive MPB induced disturbances in northern and high-altitude ecosystems where they were previously absent or rare (Logan et al., 2003). This leaves forest managers challenged to find solutions to novel pest problems for which there is little historical direction or well-tested solutions (Ayres and Lombardero, 2000; Volney and Hirsch, 2005). However, utilizing ambient air temperatures to produce an effective

model of phloem temperatures would offer a more accurate picture of MPB phenology under a variety of ambient air temperature fluctuations.

In Bolstad et al. (1997) the authors develop two phloem temperature models that reconstruct hourly phloem temperatures; “lapse” and “geographic.” Both models use differing methods to calculate daily phloem temperature maxima and minima, but both connect the daily extrema using sine and exponential functions. While both models perform relatively well, they fail to address how the errors in phloem temperatures affect errors in MPB development. The magnitude of phloem temperature errors, when filtered through the non-linear MPB developmental rate curves, may not correspond to errors in MPB phenology. For our purposes, the reproduction of phloem temperatures is unnecessarily difficult. It is sufficient to construct a phloem temperature model that generates the proper net amount of developmental energy which in turn would produce suitable MPB phenology results, underscoring the purpose of developing phloem temperature models to accurately describe MPB phenology.

Using MATLAB (Math Works 2010) as a modeling tool, various methods to model northern and southern aspect phloem temperatures from ambient air temperatures are explored using with a special interest in generating phloem temperature models that induce the correct net amount of developmental energy relative to MPB phenology. Hence, MPB phenology is used as the metric of model performance. Based on models’ abilities to recreate MPB phenology, we will show that Newton’s Law of Cooling best models northern aspect phloem temperatures while the Matching model, a method that substitutes recorded phloem temperatures for predicted phloem temperatures depending on ambient temperatures, best models southern aspect phloem temperatures. Furthermore, we will show that, while these models were initially calibrated and tested in the SNRA, they also perform well in the DNF and RRR, the validation sites. With the availability to accurately predict phloem temperatures over a large elevation change and different geographic regions, we are better equipped to forecast MPB population growth and contraction. In particular, we will be better armed to monitor and protect the vital high-elevation pines as well as manage lower elevation forests in a more proactive fashion.

## 2 Methods

Six different approaches were used to model phloem temperatures from ambient air temperatures: Cosine, Sawtooth, Newton, Cosine-Exponential, Newton South and Matching. While the models vary in approach, most of the parameters are in reference to daily minimum and maximum phloem temperatures since the daily extrema form the core of most of the models. The models were parameterized using two distinct sets of data collected in the SNRA from the Ranch and Vienna sites. The Ranch temperatures (collected in 1996-1997) are fairly typical in the SNRA. The Vienna temperatures (collected in 2001-2002) are some of the warmer temperatures in the SNRA collection.

### 2.1 Phenology Metrics

The purpose of our phloem temperature models is to generate phloem temperatures which can be used to predict MPB phenology. To measure which model performed best, we examined how the results of existing phenology models differed when predicted phloem temperatures were used instead of observed phloem temperatures. Four phenology models were used for comparison: the G-Function model, which predicts the median emergence date of eggs laid on a given date; the Extended Von Foerster model, which describes the breadth and placement of the resulting emergence distribution from an observed attack distribution; the MPB Voltinism model, which describes MPB synchrony; and the R-Function model, which connects MPB phenology to population growth rate. Since each phenology model highlights a different aspect of MPB phenology, the phloem temperature model that performs well using all four phenology model metrics captures a large spectrum of the significant components of phloem temperatures that drive MPB populations.

#### 2.1.1 G-function

The first phenology metric used is based on the G-function, a circle map by which one can estimate the oviposition date of a given generation based “directly and uniquely on the oviposition date of the previous generation” (Powell and Logan, 2005). So given a series of temperatures and the set of rate curves for all the MPB developmental stages, the G-function calculates the sequence of developmental milestones, from the date of oviposition through larval instars, culminating in the emergence of the reproductive adult and oviposition of the next generation. We focused on



the G-function predictions generated over the MPB oviposition season, Julian day 152 through Julian day 245, since eggs laid outside this seasonal window will likely not survive the winter, or will pupate at an unseasonable time of year (Powell and Bentz, 2009). The G-function has one independent variable, phloem temperature. This makes it an ideal phenology model to compare the effects of varying phloem temperatures on MPB developmental timing. There are dramatic jumps that can occur in the G-function since MPB must reach certain developmental requirements before proceeding to the next life stage. This can be seen in figure 2. The result of these jumps is that small errors in phloem temperature predictions may result in massive errors in the G-function model if the predictions cause the timing of the jumps to be off. In order to measure how well each model was performing with respect to the G-function, we calculated the absolute error generated by each model over the MPB oviposition season. Specifically, the metric is expressed as

$$|G_{error}| = \sum_{j=1}^j \sum_{n=152}^{245} |G_{pred,n} - G_{obs,n}|,$$

where  $j$  is the number of trees from which phloem data was collected at the site,  $G_{pred,n}$  and  $G_{obs,n}$  correspond to the emergence days generated from predicted phloem temperatures and observed phloem temperatures for oviposition day  $n$ . Thus, larger numbers would indicate greater error. Since the  $|G_{error}|$  value often becomes large, we calculated the error relative to the  $|G_{error}|$  value achieved by the poorest performing model on both the northern and southern aspects in order to more easily compare model performance.

### 2.1.2 Extended von Foerster

The second metric used was based on the Extended von Foerster model (EvF). The von Foerster model was originally derived by McKendrick in 1926 and by von-Foerster in 1959 (McKendrick, 1926; von Foerster, 1959). In 2004, the Extended von Foerster MPB model was developed as an adaptation of the original von Foerster model accounting for variability and poikilotherm development (Gilbert et al., 2004). Given MPB developmental rate curves and a temperature series, the EvF model calculates a distribution of adult emergence for the next generation using the distributions of adult emergence in the current generation (Powell and Bentz, 2009). Errors accumulated through the other life stages will be aggregated in the adult emergence predictions as seen in figure

3. From the EvF result we calculated when the 10<sup>th</sup>, 50<sup>th</sup> and 90<sup>th</sup> percentile of the MPB population would have emerged, giving us a measurement to compare differences in the distributions. In instances when phloem data was collected from multiple trees at a site, we used the average of the respective 10<sup>th</sup>, 50<sup>th</sup> and 90<sup>th</sup> percentile dates generated by each tree’s observed phloem temperatures as the observed quantity. From the averaged emergence percentile dates,  $r^2$  values can be calculated to see how closely the distributions produced from predicted and observed phloem temperatures match.

While  $r^2$  values are the primary figure of merit in the EvF metric; comparisons between the percentile dates generated from predicted phloem temperatures and those produced from observed phloem temperatures offer further insight. Specifically, an over-prediction of developmental energy by a model incorrectly inserts excessive energy into MPB development and generally causes a premature occurrence of the emergence percentiles whereas a consistent under-prediction would result in the predicted emergence percentiles occurring later. Thus, the  $r^2$  value describes the models’ overall performance and the timing of the emergence percentiles imply why a model may be performing poorly.

### **2.1.3 R-function**

The third metric we used was based on the R-function, a MPB-specific model introduced by Powell and Bentz (2009), which uses the Extended von Foerster model along with an effectiveness threshold, or the minimum number of MPB needed to attack a tree per day in order to successfully colonize it, to predict a discrete growth rate. Like the G-function and EvF phenology models, the R-function depends on phloem temperatures, but also gives different results depending on whether northern or southern aspect phloem temperatures are used. To compare performance between the various phloem temperature models we calculated  $r^2$  values using the growth rate induced by predicted phloem temperatures and the growth rates generated by the observed phloem temperatures at a given site across all years of data. In the instances when phloem data was collected from multiple trees at a site, we averaged the growth rates generated by each tree’s observed phloem temperatures. An over-prediction of developmental energy results in an elevated growth rate while an under-prediction yields a lower growth rate. So, while the growth rate indicates the reason a model performs poorly, the  $r^2$  value indicates the model’s overall performance.

#### 2.1.4 MPB Voltinism

Like the previous phenology metrics, the MPB Voltinism phenology metric is also driven by phloem temperatures. The MPB Voltinism phenology metric iterates the same temperatures over and over while utilizing the G-function to estimate MPB voltinism, or the number of generations per year. For example, a voltinism prediction of  $\frac{1}{2}$  would imply one generation per two years while a prediction of  $\frac{4}{3}$  indicates four generations per three years. Univoltine (or one generation per year) behavior is key for the MPB to be adaptive to its thermal environment (Powell and Logan, 2005). MPB voltinism produced from the model form bands of varying stability; fractional bands tend to be more unstable (figure 4). So, if the MPB Voltinism prediction generated from observed phloem temperatures is centered in a stable univoltine band, then it may take very poor phloem temperature predictions to yield a different result. On the other hand, if the data produces voltinism in an asynchronous fractional voltinism band, then small deviations in phloem predictions from observed phloem temperatures can yield drastically different voltinism predictions. Hence, the sensitivity of the MPB Voltinism model varies dependent upon whether the actual voltinism is univoltine or fractional. To assess goodness of fit with respect to the MPB Voltinism, the frequency that the predicted phloem temperatures induced the exact voltinism generated by the observed phloem temperatures was calculated. In the cases where phloem data was gathered from multiple trees at a given site, we concluded that the predicted phloem temperatures induced the correct voltinism if any of the observed phloem temperatures generated the same voltinism. Additional insight is gleaned by noting that a general over-prediction of developmental energy, which would reduce development time, produces a greater (more generations/year) voltinism than the observed temperatures generates; consistent under-prediction, which increases development time, usually results in a lesser (fewer generations/year) voltinism.

#### 2.1.5 Use of Phenology Models

By using the G-function, Extended von Foerster, R-function and MPB Voltinism phenology models to compare the various phloem temperature models' results, we are able to see how closely the phloem temperature models represent actual phloem temperature relative to MPB phenology. Since each phenology metric focuses on a different aspect of MPB phenology, a phloem temperature model

that performs well under each of the phenology metrics would capture the main aspects of phloem temperatures that drive MPB phenology.

## 2.2 Phloem Temperature Models

Since air temperatures are relatively abundant but do not readily induce correct MPB phenology and given that phloem temperatures are rarely observed and recorded, we need to be able to convert measured ambient temperatures into phloem temperatures in order to increase the usefulness of the existing MPB phenology models. As seen in figure 1, north-side and south-side phloem temperatures can be quite different. The difference between northern and southern aspect phloem temperatures translates into vastly different phenology predictions since the southern aspect experiences greater solar input which generally results in a quicker MPB development when compared to the northern aspect. Also, some of the phenology models use different parameters depending on whether north-side or south-side phloem temperatures are used (Powell and Bentz, 2009). To account for the difference between aspects, the northern and southern aspect phloem temperatures were modeled separately.

On both the north and south sides of the bole, we first linked daily minimum and maximum ambient temperatures to daily minimum and maximum phloem temperatures to make the initial connection between ambient and phloem temperatures. Once the daily extremes were modeled, we used a variety of functions (linear, sinusoidal, exponential) to fill in the remaining phloem temperatures, thus creating the Sawtooth, Cosine and Cosine-Exponential phloem temperature models. Also from the ambient temperatures, we applied Newton’s law of cooling to generate phloem temperatures, forming the basis for the Newton and Newton South models. Lastly, we match daily minimum and maximum ambient temperatures to an archive of ambient and phloem temperatures in the Matching model. Through these models we are able to explore many ways to generate phloem temperatures from ambient temperatures.

### 2.2.1 Phloem Maxima and Minima

At their core, most of the methods we devised to predict phloem temperatures used a linear regression between minimum daily ambient temperatures,  $A_{min}$  and minimum daily phloem temperatures,  $P_{min}$ , as well as maximum daily ambient temperatures,  $A_{max}$  and maximum daily phloem

temperatures,  $P_{max}$ . Minimum ambient and minimum phloem temperatures have a very strong positive on both the northern and southern aspects of the bole (figures 5 and 6). As we see, the regression line, or linear fit, provides a model for predicting daily northern bole aspect minimum phloem temperatures from daily ambient temperatures of the form

$$P_{min,N} = 0.9743A_{min} + 1.468 \quad (\text{Ranch, figure 5a}),$$

$$P_{min,N} = 1.060A_{min} + 3.092, \quad (\text{Vienna, figure 5b}),$$

when parameterized with the Ranch and Vienna data sets respectively. As we see in figures 5a and 5b the data is tightly distributed about the regression line as is indicated by the respective  $r^2$  values of 0.99 and 0.98.

On the southern aspect of the bole, the minimum temperature regression lines are of the form

$$P_{min,S} = 0.9892A_{min} + 1.552 \quad (\text{Ranch, figure 6a}),$$

$$P_{min,S} = 1.067A_{min} + 2.826 \quad (\text{Vienna, figure 6b}),$$

when parameterized with the Ranch and Vienna data sets respectively. Again, in figures 6a and 6b, we see tight distributions about the regression lines under the Ranch and Vienna parameterizations as is evident by respective  $r^2$  values of 0.99 and 0.98.

The data for maximum temperatures suggests a similar relationship to the minimum temperatures on the north side. Hence, maximum daily phloem temperatures on the northern bole aspect were again modeled using linear regression. These lines were of the form

$$P_{max,N} = 1.026A_{max} - 0.2055 \quad (\text{Ranch, figure 7a}),$$

$$P_{max,N} = 0.8591A_{max} + 0.4929 \quad (\text{Vienna, figure 7b}),$$

when parameterized with the Ranch and Vienna parameterizations respectively. Similar to the relationship between minimum phloem and ambient temperatures, the data for northern bole aspect daily maximum phloem and ambient temperatures, under the Ranch and Vienna parameterizations, are tightly distributed around the respective regression lines as is evident by respective  $r^2$  values of

0.99 and 0.98.

With the exception of the south side maximum phloem temperatures, daily maximum and minimum phloem temperatures have thus far been modeled from the ambient maximum and minimum temperatures using linear regression on both aspects of the bole. As was done with the other extrema, modeling the maximum daily phloem temperatures in the southern aspect through regression techniques resulted in models of the form

$$P_{max,S} = 1.0256A_{max} + 3.5583 \quad (\text{Ranch, figure 8a}),$$

$$P_{max,S} = 0.61752A_{max} + 11.917 \quad (\text{Vienna, figure 8b}),$$

when parameterized with the Ranch, and Vienna parameterizations respectively. Unlike the previous extrema, the distributions about the regression lines are not nearly as tight as is evident by the respective  $r^2$  values of 0.82 and 0.41. This error is problematic since there are many days when, according to the developmental rate curves described in Jenkins et al. (2001), little development occurs based on low  $P_{max,S}$  but, the observed temperatures indicate rapid MPB development. While the distribution is well formed beneath the regression line, it appears to be much more random above the line thus, it is hard to predict an accurate daily maximum phloem temperature on the southern aspect.

In order to better predict daily maximum phloem temperatures on the southern bole we acknowledged that the actual maximum daily phloem temperature,  $P_{max,obs}$  was equal to the predicted maximum daily phloem temperature,  $P_{max,S}$ , plus an error term,  $\varepsilon$ . The appended term,  $\varepsilon$ , is attributed to the additional radiant solar input received on the southern aspect mentioned in Powell and Bentz (2009). Thus,  $P_{max,obs} = P_{max,S} + \varepsilon$ ; so,  $\varepsilon = P_{max,obs} - P_{max,S}$ . To best describe the  $\varepsilon$  we calculated  $P_{max,obs} - P_{max,S}$  from the training data set. These residuals,  $\varepsilon = P_{max,obs} - P_{max,S}$ , (figure 9) were then normalized to display relative frequencies. We then have the proportion of cases that fall into each of several categories, or the probability distribution function (PDF),  $f(e)$ , where  $e$  is the calculated error. By summing the relative frequencies the corresponding cumulative distribution function,  $F(e)$  can be calculated as seen in figure 10. Now, simply set  $F(e) = u$  where  $u \in [0,1]$  and draw 365 random  $u$  values, one for each day of the year, from the Uniform(0,1) distribution. By computing  $F^{-1}(u)$  to get  $e$  values, which are draws from  $f(e)$ , the PDF, the

observed error can be estimated. In this manner the observed variability in predicting maximum phloem temperatures can be simulated stochastically.

### 2.2.2 Sawtooth

With the daily extremes estimated, we connected the sequences of predicted phloem minima ( $P_{min}$ ) to the appropriate predicted phloem maxima ( $P_{max}$ ) using simple straight lines, creating the Sawtooth model (figure 11), which yields hourly phloem temperature predictions. A similar model was used in Hicke et al. (2006). The authors in the Hicke version, as a substitute for phloem temperatures in MPB phenology models, connect predicted ambient maxima and minima with a sawtooth pattern. However, as we see in figure 1, ambient temperatures can vary greatly from phloem temperatures. Hence, basing the extremes of the Sawtooth model on predicted phloem temperature extremes we mimic more of the driving influence of MPB phenology.

Since the models for maximum and minimum phloem temperatures were northern and southern aspect specific, this process left us with two Sawtooth models - one for the northern aspect and one for the southern aspect. So, let  $P_{max/min}^d$  signify the predicted maximum or minimum phloem temperature on Julian day  $d$  and let  $t$  be the Julian hour. Then the Sawtooth model is of the form

$$P_t = \begin{cases} \left( \frac{P_{max}^d - P_{min}^d}{t_{max}^d - t_{min}^d} \right) (t - t_{max}^d) + P_{max}^d & \text{for } t \in [t_{min}^d, t_{max}^d), \\ \left( \frac{P_{min}^{d+1} - P_{max}^d}{t_{min}^{d+1} - t_{max}^d} \right) (t - t_{max}^d) + P_{max}^d & \text{for } t \in [t_{max}^d, t_{min}^{d+1}), \end{cases} \quad (1)$$

where  $t_{max/min}^d$  is the predicted Julian hour at which the maximum or minimum phloem temperature occur on Julian day  $d$ . The hour when the phloem extrema occurs,  $t_{max/min}^d$ , is the same hour at which the maximum or minimum ambient temperature occurs. The Sawtooth models are appealing since they are elementary and easy to implement.

### 2.2.3 Cosine

In an effort to match the curvature exhibited by the data we used a Cosine model which connects the  $P_{min}$ 's to the appropriate  $P_{max}$ 's with a cosine wave (figure 12). The Cosine model is of the

form

$$P_t = \begin{cases} \frac{1}{2} (P_{max}^d + P_{min}^d) + \frac{1}{2} (P_{max}^d - P_{min}^d) \cos \left[ \pi + \frac{\pi(t - t_{min}^d)}{t_{max}^d - t_{min}^d} \right] & \text{for } t \in [t_{min}^d, t_{max}^d), \\ \frac{1}{2} (P_{max}^d + P_{min}^{d+1}) + \frac{1}{2} (P_{max}^d - P_{min}^{d+1}) \cos \left[ \frac{\pi(t - t_{max}^d)}{t_{min}^{d+1} - t_{max}^d} \right] & \text{for } t \in [t_{max}^d, t_{min}^{d+1}). \end{cases} \quad (2)$$

A similar model was presented in Powell and Bentz (2009) as well as Hicke et al. (2006), but in both instances the sinusoidal functions connect ambient extremes. The Cosine models are pleasing for two reasons: they are simple and they intrinsically exhibit the sinusoidal nature of the data. On the other hand, they also tend to lock into under or over prediction cycles we see in figure 12.

#### 2.2.4 Newton: Northern Aspect

In Tran et al. (2007) the authors successfully use Newton’s Law of Cooling to assess how much buffering tree bark provides from minimum ambient temperatures. Given that Newton’s Law of Cooling is frequently used to describe how ambient temperatures affect a given object’s temperature, we used Newton’s Law of Cooling to specifically target northern aspect phloem temperatures. According to Newton’s Law of Cooling, the rate of change in phloem temperature is proportional to the difference between the current phloem temperature and the ambient temperature. We then have

$$\frac{dP}{dt} = k(P - A)$$

where  $A$  is the ambient temperature,  $P$  is the phloem temperature and  $k$  is the rate of temperature transfer. The differential  $\frac{dP}{dt}$  was estimated with  $\frac{P(t+1) - P(t)}{\Delta t}$ , a finite difference where  $P(t)$  corresponds to phloem temperature at hour  $t$  and the parameter  $k$  was estimated using linear regression. From the regression estimations,  $k = 0.5258$  and  $k = 1.3357$  under the Vienna and Ranch parameterizations respectively. This led to the Newton models

$$P(t + \Delta t) = P(t) + k[P(t) - A(t)]\Delta t. \quad (3)$$

We take  $\Delta t = 1$  since our minimum time step is 1 hour. As seen in figure 13, the Newton model, while not precisely correct, tracks northern aspect phloem temperatures very well. However, one immediate draw-back to the Newton model is the necessity of an hourly ambient temperature record



whereas the previous models, Sawtooth and Cosine, only need ambient maxima and minima.

### 2.2.5 Cosine-Exponential: Southern Aspect

As seen in figure 1, southern aspect phloem temperatures can differ greatly from both ambient and northern aspect phloem temperatures. The Cosine-Exponential model is designed to better match the shape of the southern aspect phloem temperatures. This model is similar to the Sawtooth and Cosine models described above in that it is an attempt to connect  $P_{min,S}$  to  $P_{max,S}$  in a manner that best matches the data. So, the Cosine-Exponential model is of the form

$$P_t = \begin{cases} \frac{1}{2} (P_{max}^d + P_{min}^d) + \frac{1}{2} (P_{max}^d - P_{min}^d) \cos \left[ \pi + \frac{\pi(t - t_{min}^d)}{t_{max}^d - t_{min}^d} \right] & \text{for } t \in [t_{min}^d, t_{max}^d), \\ (P_{max}^d) \left( \frac{P_{min}^{d+1}}{P_{max}^d} \right)^{\frac{1}{(t_{min}^{d+1} - t_{max}^d)(t - t_{max}^d)}} & \text{for } t \in [t_{max}^d, t_{min}^{d+1}), \end{cases} \quad (4)$$

using a cosine curve to represent the daytime hours, connecting predicted daily minimum phloem temperatures to predicted daily maximum phloem temperatures and an exponential curve to denote the night hours, connecting predicted phloem maxima to minima (figure 14). As seen in figure 14, when the predicted maximum and minimum phloem temperatures are well aligned, then the model appears to have a shape similar to phloem temperatures.

### 2.2.6 Newton South: Southern Aspect

When we implemented the Newton model on the southern aspect, it was evident by its poor performance that phloem temperatures on that side did not follow Newton's Law of Cooling. To rectify the difference a parameter,  $I$ , was added to the Newton model to account for the additional error outside Newton's Law of Cooling, giving

$$\frac{dP}{dt} = k(P - A) + I.$$

The parameter  $k$  (rate of temperature transfer) was estimated in the Newton model for the northern aspect and is unchanged in the Newton South model since the premise of the model is that  $I$  is the difference between what is predicted through Newton's Law of Cooling and the observed phloem

temperatures. So, in its discrete form, the Newton South model is

$$P(t + 1) = P(t) + k[P(t) - A(t)]\Delta t + I_t\Delta t. \quad (5)$$

Residuals were used to generate a cumulative distribution function from which the hourly error parameter,  $I$ , was inverse-sampled. Better results were achieved by restricting the available error values from which to draw to non-negative values (i.e.  $I_j \geq 0 \forall j$ ). As with the Newton model, the Newton South model is more sophisticated than the methods of simply connecting the dots, however, it also involves more parameters than the Sawtooth, Cosine and Cosine-Exponential models discussed above. Furthermore, due to the randomly selected error parameter,  $I$ , added to the hourly predictions, the predicted phloem temperatures appear more jagged than the actual phloem temperatures. This can be seen in figure 15.

### 2.2.7 Matching Model: Southern Aspect

The last model we devised to estimate southern aspect phloem temperatures acts on the idea that similar ambient temperatures will produce similar phloem temperature. Since the USDA Forest Service’s Rocky Mountain Research Station Forestry Sciences Laboratory in Logan, UT has collected hourly phloem temperatures for years, there is a relatively large collection of phloem temperatures along with their corresponding air temperatures. So, to generate a prediction of hourly phloem temperatures for Julian day  $d$  that occurred under air temperature conditions where the minimum air temperature for day  $d$ ,  $A_{min}^d$ , the maximum air temperature for day  $d$ ,  $A_{max}^d$ , and the minimum air temperature for day  $d + 1$ ,  $A_{min}^{d+1}$ , are all known, the Matching model simply searches the archived set of daily ambient sequences of “*minimum, maximum, minimum*” for the closest match (based on sum of squares). It then returns the archive’s corresponding phloem temperatures as predicted phloem temperatures for Julian day  $d$ . In the event that there is more than one sequence of daily ambient extremes that matches best, the model chooses at random. Results of this model can be seen in figure 16. The highlight of the Matching model is that it returns actual phloem data and hence its predictions have the shape of phloem temperatures that occurred under similar ambient conditions.

## 3 Results

### 3.1 Results: SNRA

To test the various phloem temperature models, the phenology models (G-Function, R-Function, Extended von Foerster and MPB Voltinism) were first executed using northern and southern aspect phloem temperatures from 11 years and 6 locations within the SNRA as the input argument. This output was then compared with results generated with predicted phloem temperatures, parameterized using Ranch and Vienna data (figure 17).

#### 3.1.1 Cosine: Northern Aspect

Since the Cosine model is northern and southern aspect specific, the results for this model are also northern and southern aspect specific. As is seen in tables 1 and 2, the Cosine model did not perform well with respect to any phenology metric. Rather, the Cosine model distinctly over-estimated the net developmental energy from northern aspect phloem temperatures under both parameterizations. This is seen in the R-function's averaged growth rate and the averaged emergence percentile dates produced from the EvF metric. The high cumulative absolute error calculated in the G-function metric along with the poor MPB Voltinism metric performance (tables 3 and 4) also imply that the Cosine model markedly over-predicts the net developmental energy. Hence, the Cosine model decisively over-estimates developmental energy and thus, performs poorly by every phenology metric.

#### 3.1.2 Cosine: Southern Aspect

On the southern aspect, under the Vienna parameterization, the Cosine model had a tendency to conspicuously over-predict the developmental energy from southern aspect phloem temperatures and thus, did not perform well by any of the phenology metrics (table 1). This over-prediction is especially evident in the MPB Voltinism and EvF metrics. The voltinism predictions tend to be greater than those induced by observed phloem temperatures (table 5) and the averaged emergence percentile timing, from the EvF metric, is early (table 1). Additionally, the high error seen in the G-function is due to the predicted phloem temperatures inducing beetle emergence dates that occur before the dates produced from observed phloem temperatures, another indication that the

Cosine model is over-predicting the developmental energy. While the averaged growth rate from the R-function metric would typically indicate an under-prediction of developmental energy, the dates of the averaged emergence percentiles produced by the Cosine model are unseasonably early; thus, driving down the growth rate. So, in this case the low averaged growth rate in the R-function metric is actually a reflection of a drastic over-estimation of developmental energy. Hence, every metric implies that the Cosine model performs poorly due to an over-prediction of developmental energy when using the Vienna parameterization.

By contrast, under the Ranch parameterization the Cosine model noticeably under-predicted the overall developmental energy on the southern aspect. Thus, it failed to perform well by any metric (table 2) and the under-prediction is apparent in every metric. The growth rate from the R-function is lower and the averaged emergence percentile dates occur later than those produced from observed phloem temperatures (table 2). Furthermore, the cumulative absolute error calculated in the G-function metric along with the poor MPB Voltinism metric performance (tables 2 and 5) imply that the Cosine model markedly under-predicts the developmental energy on the southern aspect when using the Ranch data to estimate maxima and minima.

### **3.1.3 Sawtooth: Northern Aspect**

On the northern aspect, under the Ranch and Vienna parameterizations, the Sawtooth model did not perform well in nearly every metric (tables 1 and 2). Rather it tended to over-predict developmental energy. This is seen in the R-function's higher averaged growth rate and the early occurring averaged emergence percentile dates in the EvF metric. Furthermore, the high cumulative absolute error calculated in the G-function metric is due to emergence dates occurring too early. While the Sawtooth model frequently matched univoltine predictions generated from observed phloem temperatures, it generally caused an over-estimate in the MPB Voltinism metric (tables 3 and 4). In all, it is apparent that the Sawtooth model markedly over-predicts the developmental energy on the northern aspect and thus, performed poorly.

### **3.1.4 Sawtooth: Southern Aspect**

Under the Vienna parameterization, it appears that the Sawtooth model over-predicts developmental energy and thus performed poorly by nearly every metric. While the  $r^2$  value generated in the

EvF metric shows the model captures over 50% of the data’s variability, the averaged emergence percentiles, which are early, indicate that the model is noticeably over-predicting developmental energy (table 1). Similarly, the voltinisms produced from predicted phloem temperatures in the MPB Voltinism metric are higher than those generated from observed phloem temperatures (table 5) as is the averaged growth rate produced in the R-function metric (table 1). Hence, the Sawtooth model markedly over-predicts developmental energy received on the southern aspect and thus performs poorly.

Contrarily, as seen in table 2, the Sawtooth model noticeably under-predicts the developmental energy received on the southern aspect under the Ranch parameterization and thus, performs poorly in all of the metrics. From tables 2 and 6 it is seen that both the averaged growth rate and voltinisms generated from predicted temperatures are less than those produced from observed phloem temperatures. Additionally, the predicted phloem temperatures induced averaged emergence percentile dates that occurred after those produced from observed phloem temperatures; this delay is also reflected in the absolute error seen in the G-function metric (table 2). Consequently, the Sawtooth model under-estimates developmental energy under the Ranch parameterization.

### **3.1.5 Newton: Northern Aspect**

Under both the Vienna and Ranch parameterizations the Newton model performed well in nearly every metric. In particular, as seen in tables 1 and 2 the Newton model does not markedly over- nor under-estimate the net developmental energy relative to MPB. While some of the metrics imply an over-estimation, others imply an under-estimation by the Newton model, i.e., the EvF and R-function metrics under the Ranch parameterization (table 2). More importantly, the Newton model produced phloem temperatures that generated MPB phenology similar to the MPB phenology produced from observed phloem temperatures.

The Newton model performed particularly well under the Ranch parameterization. The cumulative sum of absolute error in the G-function results is decidedly less than the errors produced by other models. Additionally, the Newton model generated the highest  $r^2$  values with respect to the EvF and R-function metrics and produced univoltine predictions whenever the observed temperatures did in the MPB Voltinism metric (table 4). Hence, by every metric, the Newton model under the Ranch parameterization generated the most accurate northern aspect phloem temperatures

relative to MPB phenology.

### **3.1.6 Newton South: Southern Aspect**

Under the Vienna and Ranch parameterizations, the Newton South model generated accurate phloem temperatures relative to MPB phenology. In both cases the Newton South model generated univoltine predictions whenever observed phloem temperatures produced a univoltine solution in the MPB Voltinism metric (tables 5 and 6). With respect to the G-function, the Newton South model performed well in each case (tables 2 and 3) and, in both cases, the emergence dates generated by predicted phloem temperatures were neither consistently greater than nor less than those calculated from observed phloem temperatures. Similarly, from the EvF results we see that the model performed well under both the Vienna and Ranch parameterizations, giving accurate phloem temperatures relative to MPB phenology.

### **3.1.7 Cosine Exponential: Southern Aspect**

The Cosine-Exponential model, when using the Ranch parameterization, noticeably under-predicted the developmental energy on the southern aspect, resulting in poor performance in nearly every metric (table 2). While every metric indicates that the model performs poorly, the late occurring averaged emergence percentile dates and lower than expected growth rate from the EvF and R-function metrics indicate that the model under-predicts developmental energy (table 2). Similarly, the absolute error in the G-function, due largely to a later occurrence of adult emergence dates, and the voltinisms produced from the Cosine-Exponential model suggest that the net developmental energy is under-predicted (table 6). Hence, under the Ranch parameterization, every metric implies that the Cosine-Exponential inadequately represents southern aspect phloem temperatures.

However, under the Vienna parameterization, the Cosine-Exponential model markedly over-predicted the net developmental energy. From the higher than expected voltinisms in table 5 and the earlier than expected averaged emergence percentile dates in the EvF metric (table 1), it appears that the Cosine-Exponential model over-predicts the net developmental energy. While the R-function results in table 1 generally suggest an under-prediction of net developmental energy, in this instance the averaged growth rate is likely depressed due to unseasonably early adult emergence as is evidenced by the EvF metric. This implies a drastic over-estimation of the net developmental

energy. Similarly, the absolute error calculated in the G-function metric is due to a premature occurrence of emergence dates. Thus, the Cosine-Exponential model does not produce accurate southern aspect phloem temperatures relative to MPB phenology.

### **3.1.8 Matching: Southern Aspect**

While the Matching model performed well under both the Vienna and Ranch parameterizations, the phloem temperatures produced using the Ranch parameterization generated especially accurate MPB phenology. Under both parameterizations the model generated relatively low error in the G-function while generating high  $r^2$  values in the EvF and R-function metrics (tables 1 and 2). However, only under the Ranch parameterization did the Matching model successfully produce univoltine solutions, a distinct thermal cue, whenever the observed phloem temperatures did (tables 5 and 6) despite implications from the EvF and R-function metrics that the model did not produce sufficient thermal input under the Ranch parameterization (table 2). Hence, the Matching model performed well under both parameterizations.

## **3.2 Results: Railroad Ridge**

From the SNRA results we see that the Newton model best predicts northern aspect phloem temperatures while the Matching and Newton South models best predict southern aspect phloem temperatures (tables 1 and 2). To further test these more successful phloem temperature models we compared the results of the phenology models (G-Function, R-Function, Extended von Foerster and MPB Voltinism) generated from predicted and observed phloem temperatures. These temperatures were gathered at the Railroad Ridge (RRR) site, an area that differs greatly from the SNRA. Thus, we can ascertain whether the relative success in predicting phloem temperatures seen in the SNRA can be extended to an area that differs in elevation, temperature and host species.

### **3.2.1 Newton: Northern Aspect**

The Newton model, under the Vienna and Ranch parameterization, accurately reproduced phloem temperatures relative to MPB phenology. Under both parameterizations, an  $r^2$  value could not be calculated with respect to the R-function since the growth rate returned by the Newton model was always 0. This however, exactly matched the results produced from observed temperatures in

all but one year. Hence, the model performs well with respect to the R-function though there is an indication that phloem temperatures may be under-predicted (tables 7 and 8). Similarly, the observed temperatures never caused a univoltine prediction; the Newton model however, caused a match 50%-62.5% of the time, a good result. Additionally, the EvF metric shows the model performs well and accurately predicts the net developmental energy. Thus, while the Newton model may under-predict the net thermal input, it performs best with respect every metric.

### **3.2.2 Newton South: Southern Aspect**

The Newton South model, under both parameterizations, over-estimated the net developmental energy. In the MPB Voltinism metric the Newton South model produced voltinism predictions consistently greater than those generated from observed temperatures. Similarly, the averaged emergence percentile dates calculated in the EvF phenology metric were consistently early, signaling that developmental energy is over-predicted (tables 7 and 8). Based on the  $r^2$  values generated in the R-function metric, it appears that the model performs perfectly with respect to the R-function. However, the averaged growth rates seen in tables 7 and 8 imply that the Newton South model again over-estimates the net developmental energy. Additionally, the G-function metric indicates that the Newton South model over-predicts developmental energy since the error is due in large part to emergence dates generated from predicted phloem temperatures occurring before emergence dates calculated from observed phloem temperatures. Hence, the RRR results suggest that the Newton South model generally over-estimates developmental energy gained from southern aspect phloem temperatures.

### **3.2.3 Matching: Southern Aspect**

Like the Newton South model, the Matching model appears to over-estimate developmental energy gleaned from phloem temperatures at the RRR site under the Vienna and Ranch parameterizations. From tables 7 and 8 we see that the Matching model rarely induced a voltinism match. Instead, the Matching model generated voltinisms greater than those calculated from observed phloem temperatures in nearly every instance, thus implying that the Matching model over-estimated developmental energy. While the  $r^2$  values produced in the EvF and R-function metrics indicate adequate model performance, the averaged growth rates and the averaged emergence percentile dates imply an



over-estimation of developmental energy by the model. This is also seen in the error calculated in the G-function indicates that the Matching model noticeably over-estimated developmental energy since the adult emergence date produced from predicted temperatures occurred earlier than expected (tables 7 and 8). So, while the Matching model was the best-performing model at the RRR site, under the Vienna and Ranch parameterizations it appears that the Matching model over-estimated the net developmental energy.

### **3.3 Results: Dixie National Forest**

To further test the more successful phloem temperature models from the SNRA, we compared the results of the phenology models generated by phloem temperatures gathered at the Cedar site in the DNF, another area that differs greatly from the SNRA, with the results calculated from phloem temperatures generated by the Newton, Matching and Newton South models.

#### **3.3.1 Newton: Northern Aspect**

The Newton model, under both the Vienna parameterizations, performed well by most metrics despite many of those metrics implying that the model under-estimates the net thermal energy. As seen in tables 9 and 10, the Newton model matched the univoltine prediction that was generated from observed phloem temperatures. Similarly, the Newton model performed well with respect to the EvF metric ( $r^2 = 1$ ). Yet, under both parameterizations, the dates of the emergence percentiles calculated from the Newton model occurred 1-4 days after the dates generated by observed temperatures. Likewise, the cumulative error calculated in the G-function metric is due to emergence dates calculated from the Newton model generally occurring 5-15 days after the dates calculated from observed phloem temperatures (tables 9 and 10). Additionally, the growth rate calculated in the R-function from the predicted temperatures is less than the averaged growth rate generated from observed temperatures. Together these results suggests that while the Newton model performs well, it also tends to under-predict the net developmental energy.

#### **3.3.2 Newton South: Southern Aspect**

Like the northern aspect models, the Newton South model performed well under both the Vienna and Ranch parameterizations at the DNF site. In both cases the Newton South model generated

a univoltine prediction in the MPB Voltinism metric that matched the voltinism produced from observed phloem temperatures. It also performed well in the EvF metric. Also, the error seen in the G-function metric is not a reflection of a clear over- or under-prediction of developmental energy. On the other hand, the growth rate derived from the Newton South model under both parameterizations implies that the net thermal input is under-estimated by the Newton South model. Hence, the metrics collectively show that the mode performs well and accurately estimates the net thermal energy which is reflected in MPB phenology.

### 3.3.3 Matching: Southern Aspect

Like the Newton and Newton South models, the Matching model also performed well at the DNF site under both parameterizations. From tables 9 and 10 we see that the Matching model produced the same voltinism generated from observed temperatures while causing a favorable  $r^2$  value in the EvF metric. Additionally, the model generated growth rates similar to the averaged growth rate produced from observed temperatures (especially under the Vienna parameterization) and caused relatively little error in the G-function. So, while under the Ranch parameterization the Matching model appears to under-predict the overall thermal energy (table 10), the model predominantly encapsulates the correct amount of thermal energy relative to MPB development at the DNF site.

## Discussion

The results from the SNRA, RRR and DNF site lead to a few additional points. First, at every site, the best phenology metric results occurred under the expected parameterizations, e.g., most of the models performed better at the warmer site (DNF) when parameterized with the warmer parameterization (Vienna). Secondly, the basic interpolation models, Sawtooth, Cosine and Cosine-Exponential, rarely performed well. Thirdly, in evaluating a phloem temperature model's effectiveness, one should use more than one of the phenology metrics. Lastly, given suitable parameterizations, the Newton model clearly yields the best northern aspect phloem temperature predictions while the Matching and Newton South models perform best on the southern aspect. With this additional insight we are better able to understand the interaction between ambient and phloem temperatures.

One insight gained is consistency in the relationship between the study site and the best parameterization for that site. In the SNRA, the best results from the phenology metrics typically occur under the Ranch parameterization (tables 1 and 2). This result aligns nicely with what one may expect since the temperatures in the SNRA are, in general, not as warm as the temperatures in the Vienna parameterization. At the cooler RRR site, the Ranch parameterization even more definitively yields the best results (tables 7 and 8). Likewise, the warmer Vienna parameterization frequently yields the best results along with the Ranch parameterization at the warmer DNF site (tables 9 and 10). Thus, cooler parameterizations appear to work better at cooler sites while the warmer parameterizations work better at warmer sites, as one may expect.

On both the northern and southern aspect, the Sawtooth, Cosine and Cosine-Exponential models did not perform especially well. This suggests that simply connecting  $P_{min}$ 's to  $P_{max}$ 's tends to eliminate aspects of phloem temperatures that are critical to MPB development. In the Sawtooth-type method put forth in Hicke et al. (2006), the authors focused specifically on the probability of producing a univoltine prediction, to measure model performance. This however, is only a small snapshot of the total MPB phenology. As we have seen, models that are able to perform well with respect to one metric may not perform well with respect to another. A suitable model needs to perform adequately in a wide range of metrics; the basic interpolation models did not do this.

Another constant seen in the results is that the Newton model, when given a suitable parameterization, predicts northern aspect phloem temperatures best in all three study sites. Due to the shade on the northern aspect, the amount of energy re-radiated onto the tree bole from the surrounding environment is minimal and can be ignored. Thus, the change in phloem temperatures is reduced to discerning the interaction between phloem temperatures and the temperature of the surrounding medium, air. This is the type of scenario in which Newton's Law of Cooling performs well. Furthermore, the results strongly suggest that northern aspect phloem temperatures follow Newton's Law of Cooling since there exists a parameterization at each locale under which the Newton model yields the best results in each of the phenology metrics. Hence, given a suitable parameterization, the Newton model best predicts northern aspect phloem temperatures.

On the southern aspect the Matching and Newton South models tended to perform best. From the SNRA, RRR and DNF results we see that the Newton model tends to perform better with respect to the G-function while the Matching model performs better with respect to the R-function,

EvF and MPB Voltinism metrics. This is likely due to the Matching model’s method that uses actual phloem temperatures from an archive as the predicted phloem temperatures. Since the predicted phloem temperatures are actual phloem temperatures that occurred under a similar ambient temperature cycle, it makes sense that MPB phenology derived from the Matching model would closely resemble MPB phenology generated from phloem temperatures.

Since the Matching model requires a phloem temperature archive along with a corresponding ambient temperature archive to function, it is not useful where no phloem record exists. In such cases the Newton South model can bridge the gap when little or no phloem temperature data is available until there is a sufficiently large set of phloem temperatures. At a minimum, one would want phloem temperatures from half of a year, e.g. mid summer through mid winter, so the Matching model could choose from an area’s full swing of temperatures. After a full year’s worth of data is collected the Matching model appears to perform better than the Newton South model.

Additionally, the ambient sequence of “min, max, min” we used in the model may not be optimal. We did try a “max, min, max” sequence as well as a quartet of extremes and a few other combinations which produced results similar to our original sequence. Clearly, the number of ways to permute the search target is monstrously large and thus, further optimization may produce increasingly suitable results.

## 4 Conclusion

While there may be additional optimization to be done with the phloem temperature models, the overall relationship between ambient and phloem temperatures is more clear. In particular, on the northern aspect phloem temperatures appear to follow Newton’s Law of Cooling, while on the southern aspect the reverse boot-strapping Matching model performs best.

In this paper we have connected ambient air temperatures to phloem temperatures using MPB phenology as the metric of model performance. Models that perform well are those from which many details of MPB phenology can be accurately predicted. We have seen that simply focusing on one aspect of MPB phenology (eg. univoltinism) ignores other aspects of model performance that can more readily distinguish model performance. While good voltinism predictions are possible using basic line, sinusoidal and exponential functions, the more sophisticated Newton’s Law of

Cooling and reverse bootstrapping methods more consistently reconstructed the total phenology produced from phloem temperatures.

With the ability to accurately predict phloem temperatures from ambient air temperatures relative to MPB phenology we can more accurately predict changes in ecosystem suitability relative to the MPB under various climate change scenarios. Hence, we are better able forecast MPB population growths and contractions which in turn allows forest managers to act in a more proactive manner.

## 5 Figures

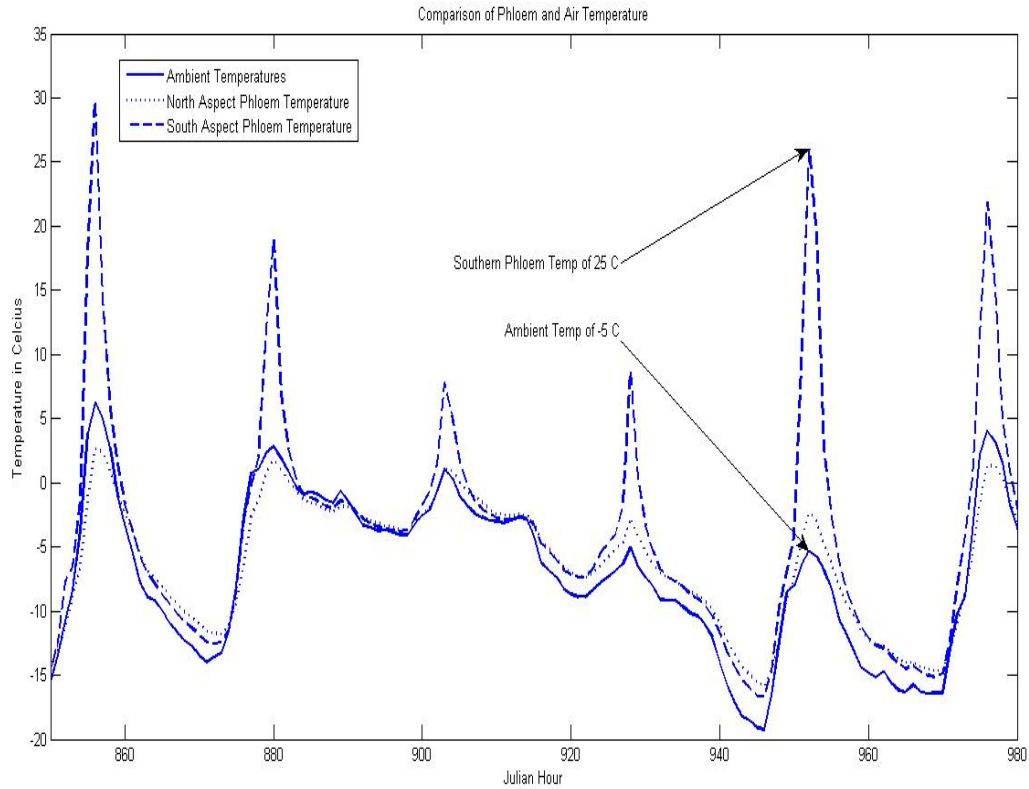


Figure 1: Comparison of ambient, northern bole aspect and southern bole aspect phloem temperatures collected at the Vienna site in SNRA. In this plot we see that the differences between northern aspect phloem temperatures and ambient temperatures are relatively small. However, differences between ambient temperatures and southern aspect phloem temperatures can be quite extreme. This difference is problematic since existing MPB phenology models generate the most accurate results when phloem temperatures are used. In the phenology models even small differences in temperatures can yield wildly different predictions due to the non-linear developmental rate curves through which the temperatures are passed. Compounding the problem, some MPB phenology models function best when driven with southern bole aspect phloem temperatures, which can differ drastically from air temperatures. However, air temperatures are much more abundant than phloem temperatures and thus, this figure underscores the need to develop a method to approximate phloem temperatures from air temperatures.

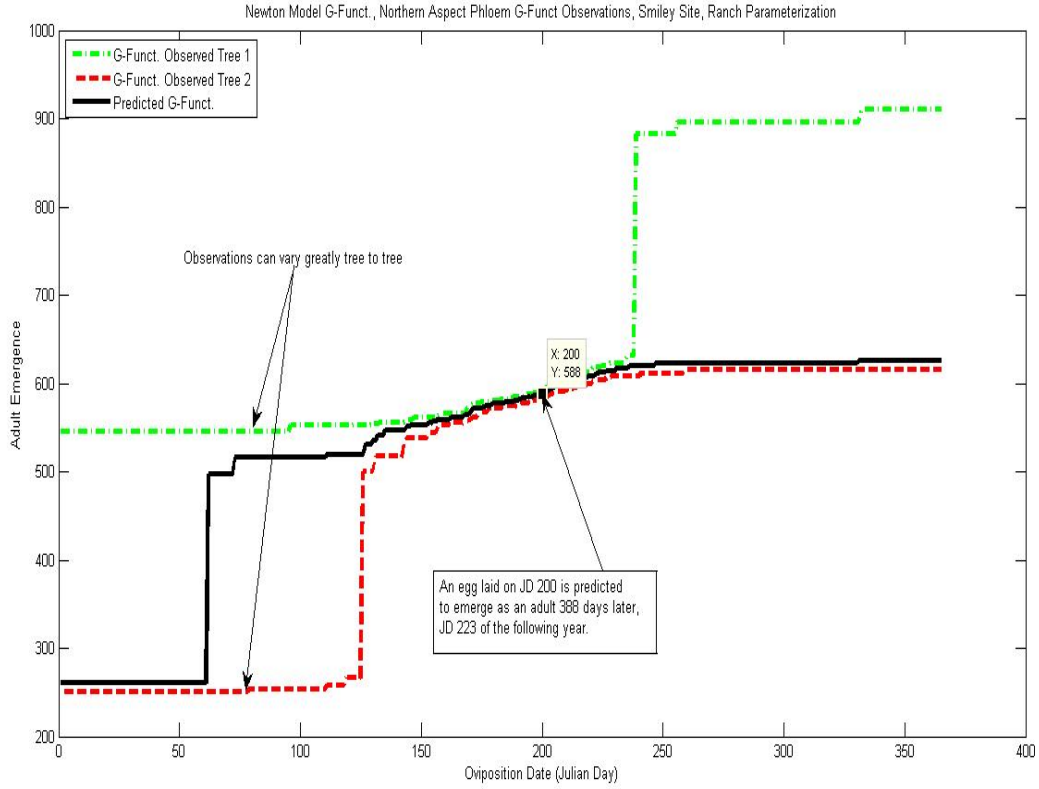


Figure 2: G-Function, which relates oviposition date to adult emergence, as generated by data collected at the Smiley site in SNRA using northern aspect phloem temperatures. The G-function is one of four phenology metrics by which one may determine how closely the MPB phenology generated from predicted phloem temperatures matches the phenology produced from observed phloem temperatures. The predicted G-Function above uses temperatures generated from the Newton model and was parameterized with data from the Ranch site in the SNRA. We see that these curves can have dramatic jumps since MPB must reach certain developmental requirements before proceeding to the next life stage. While the timing of these jumps can vary greatly from tree to tree, as seen in the figure, through the MPB seasonal oviposition window (JD 152 - JD 245) the observations are much more closely aligned. The absolute cumulative error over the seasonal oviposition window is calculated to measure how well the G-function results produced from observed and predicted phloem temperatures match.

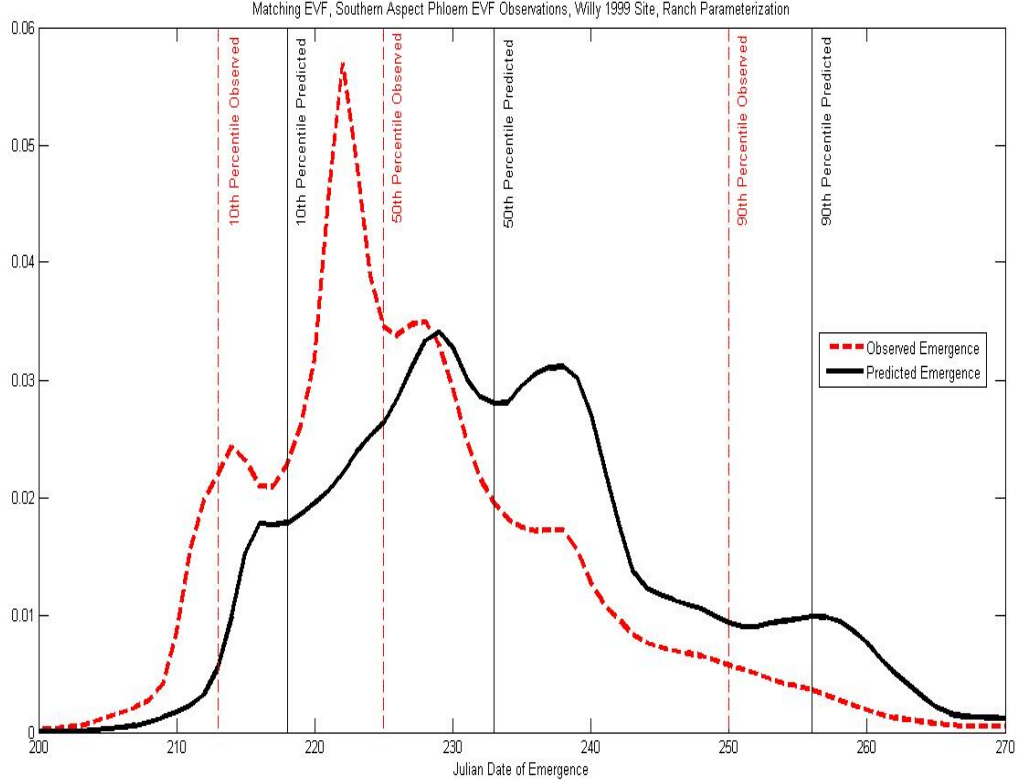


Figure 3: Plot of the Extended von Foerster phenology model (EVF), which models the distribution of adult MPB population emergence from the previous generations attack distribution (assumed to be normal). The observed EVF plot above is generated by using southern aspect phloem temperatures collected at the Willy site in SNRA in 1999. The predicted EVF plot uses predicted temperatures that were generated from the Matching model which was parameterized with 1996 SNRA data from the Ranch site. The 10<sup>th</sup>, 50<sup>th</sup> and 90<sup>th</sup> percentiles are calculated in order to measure how well the distribution generated from predicted phloem temperatures matches the distribution produced from observed phloem temperatures. Then  $r^2$  values can be calculated in order to measure how much of the variability in the data produced distribution is captured by the distribution calculated from predicted phloem temperatures. Furthermore, by comparing the Julian dates when the 10<sup>th</sup>, 50<sup>th</sup> and 90<sup>th</sup> percentiles occur, we can often see whether the phloem temperature model tends to over-or under-predict developmental energy. An over-prediction by the phloem temperature model generally causes the Julian dates of the emergence percentiles to occur before the dates produced from observed phloem temperatures. In this case that the Matching model generated predictions of adult emergence that occurred later than those generated from observed phloem temperatures thus indicating an under-prediction of developmental energy.



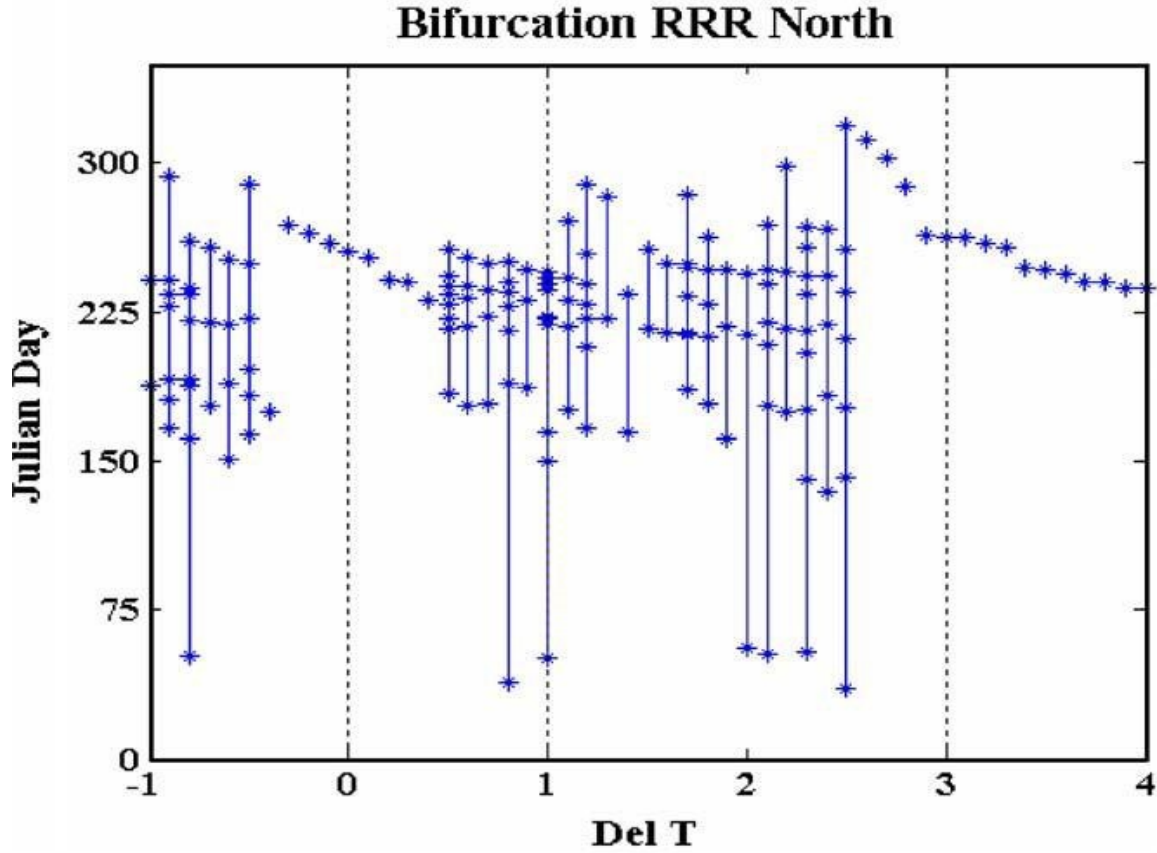
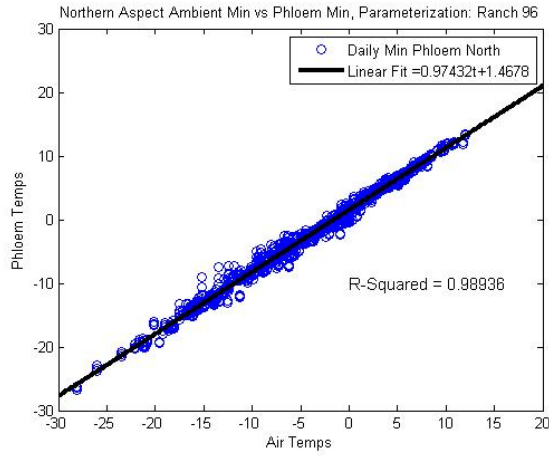
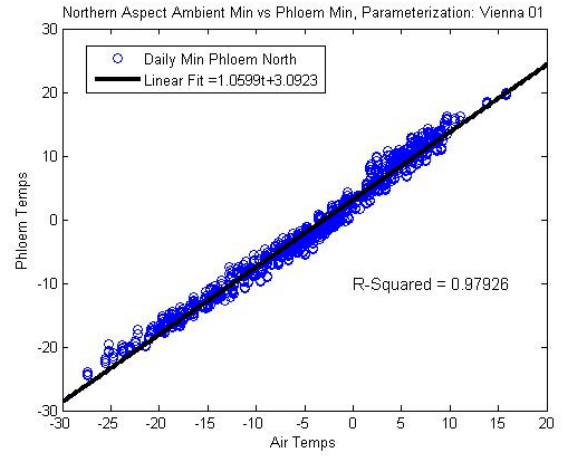


Figure 4: Bifurcation plot for annual temperatures cycle at Railroad Ridge (RRR) as it appears in Powell and Logan 2005. The vertical axis is the Julian day of MPB emergence. The  $x$ -axis shows the degrees ( $C$ ) added to (or subtracted from) hourly temperatures observed at RRR in 1995. The vertically aligned stars represent the various MPB voltinism spirals discussed in Powell and Logan 2005. For our purposes, this figure illustrates voltinism bands of varying stability produced by the MPB Voltinism metric. In particular, the vertical section intersecting the  $x$ -axis between about  $-0.25$  and  $0.5$  contains the same voltinism prediction for all those temperatures; in this case it is a semivoltine ( $1/2$ ) prediction. A larger univoltine ( $1/1$ ) band is located between  $2.75$  and  $4$ . Both the univoltine and semivoltine predictions are easily seen since there is only a single dot plotted. Multiple dots denote asynchronous fractional voltinism. So, small temperature fluctuations around  $0^\circ$  and  $3^\circ$  on the  $x$ -axis yield the same voltinism. On the other hand, the rest of the figure shows voltinism scenarios where small temperature deviations can yield drastically different predictions.

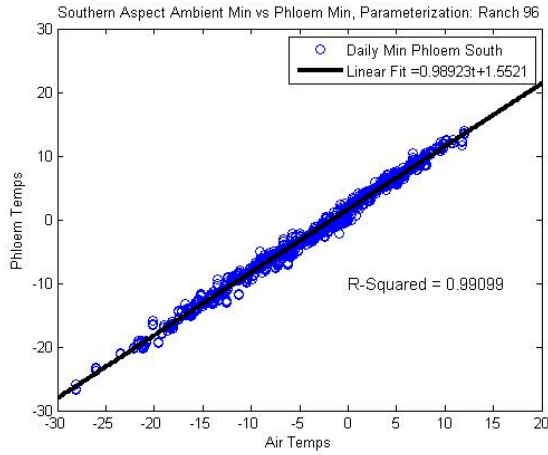


(a) Ranch:  $r^2 = 0.99$

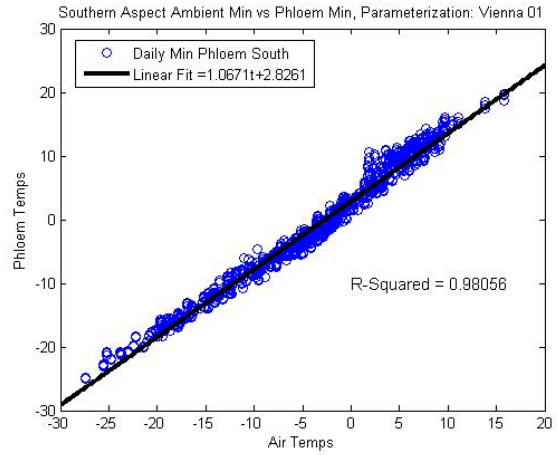


(b) Vienna:  $r^2 = 0.98$

Figure 5: Plots of the linear relationship between minimum daily phloem temperatures collected from each observed tree on the northern bole aspect and minimum daily ambient temperatures at the Ranch and Vienna sites in the SNRA respectively. As is evident by the high  $r^2$  values ( $r^2 = 0.99$  and  $0.98$  resp.), the data is tightly distributed about the regression lines. Thus, the regression lines provide an adequate means to predict daily minimum phloem temperatures on the northern bole aspect from daily minimum air temperatures. Under the Ranch parameterization the regression line has a slope of  $0.97$  and a  $y$ -intercept of  $1.47$  while under the Vienna parameterization the slope is  $1.06$  and the  $y$ -intercept is  $3.09$ . The ability to satisfactorily predict daily phloem minima, plays an important role in many of the following hourly phloem temperature models as a slew of them connect daily minima to daily maxima with various curves.

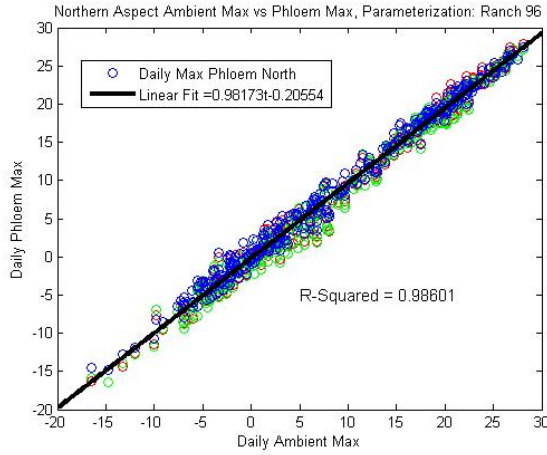


(a) Ranch:  $r^2 = 0.99$

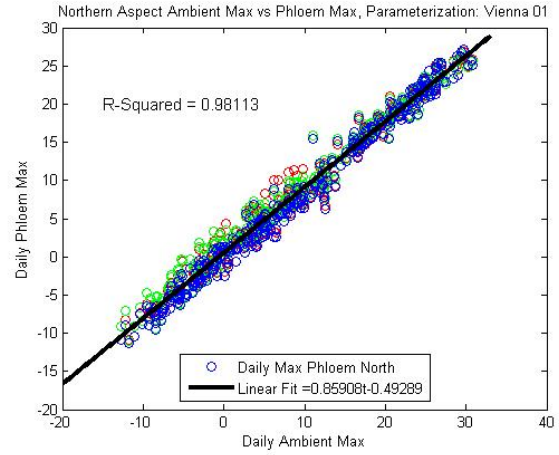


(b) Vienna:  $r^2 = 0.98$

Figure 6: Plots of the linear relationship between minimum daily phloem temperatures collected from each observed tree on the southern bole aspect and minimum daily ambient temperatures at the Ranch and Vienna sites in the SNRA respectively. Just like the on northern bole aspect, on the southern bole aspect the data is tightly distributed about the regression lines as is evident by the high  $r^2$  values ( $r^2 = 0.99$  and  $0.98$  resp.). As with the northern bole aspect, the regression lines provide sufficient means to predict daily minimum phloem temperatures on the southern bole aspect from daily minimum air temperatures. In the case of the Ranch parameterization, the regression line has a slope of 0.99 and a  $y$ -intercept of 1.55. Under the Vienna parameterization the regression line has a slope of 1.07 and a  $y$ -intercept of 2.83. Many of the following hourly phloem temperature models utilize this ability to satisfactorily predict daily phloem minima since the models often connect predicted daily phloem minima to predicted daily phloem maxima and vice versa with familiar functions.

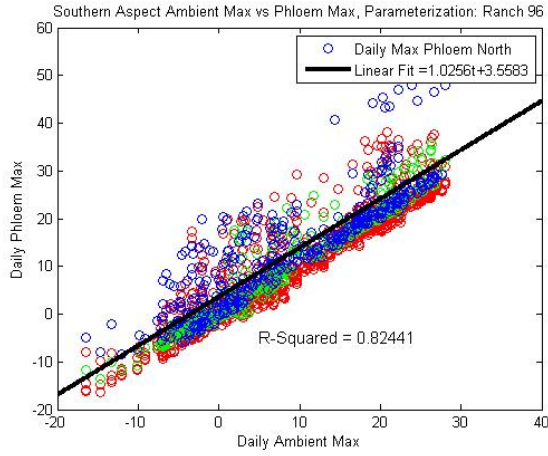


(a) Ranch:  $r^2 = 0.99$

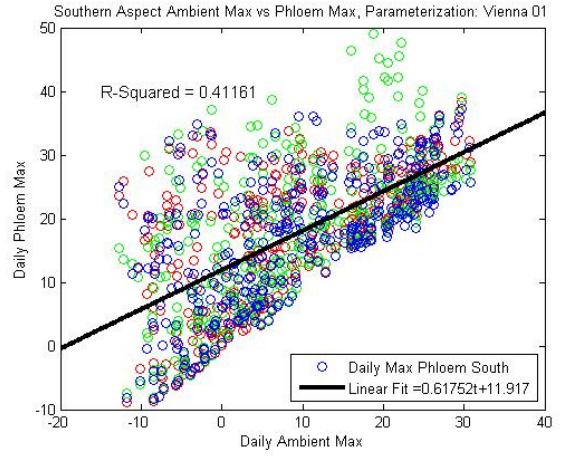


(b) Vienna:  $r^2 = 0.98$

Figure 7: Plots of the linear relationship between maximum daily phloem temperatures collected from each observed tree on the northern bole aspect and maximum daily ambient temperatures at the Ranch and Vienna sites in the SNRA respectively. As with the minima previously discussed, on the northern bole aspect the data is tightly distributed about the regression lines as is evident by the high  $r^2$  values ( $r^2 = 0.99$  and  $0.98$  resp.). Again, the regression lines provide the means to predict daily maximum phloem temperatures on the northern bole aspect from daily maximum air temperatures. In the case of the Ranch parameterization, the regression line has a slope of  $0.98$  and a  $y$ -intercept of  $-0.21$ . Under the Vienna parameterization the regression line has a slope of  $0.86$  and a  $y$ -intercept of  $-0.49$ . This model provides the daily upper-bound for the following hourly phloem temperature models. Many of the hourly phloem temperature models connect predicted daily phloem minima to predicted daily phloem maxima and vice versa, thus emphasizing the importance of this daily phloem maximum temperature model.



(a) Ranch:  $r^2 = 0.82$



(b) Vienna:  $r^2 = 0.41$

Figure 8: Plots describing the much weaker linear relationship between maximum daily phloem temperatures collected from each observed tree on the southern aspect of the bole and maximum daily ambient temperatures at the Ranch and Vienna sites in the SNRA respectively. In each of the previous cases the distributions about the regression line were very tight with  $r^2$  values between 0.98 and 0.99. Here we see that the distributions are much looser with  $r^2$  values of 0.82 and 0.41 respectively, relatively poor results. In this case, the regression line alone is not sufficient to predict daily phloem maximum temperatures on the southern bole aspect, but it does still form the base of a more successful model that follows. Under the Ranch parameterization the regression line is similar to those previously discussed with a slope of 1.02 and a  $y$ -intercept of 3.56. However, under the Vienna parameterization, the line is drastically different with a slope of 0.62 and a  $y$ -intercept of 11.92. The difference in the regression line equations underscores the greater variability seen in the data on the southern bole aspect. This increased variability, in turn, increases the difficulty of producing a suitable model for daily maximum phloem temperatures on the southern bole aspect.

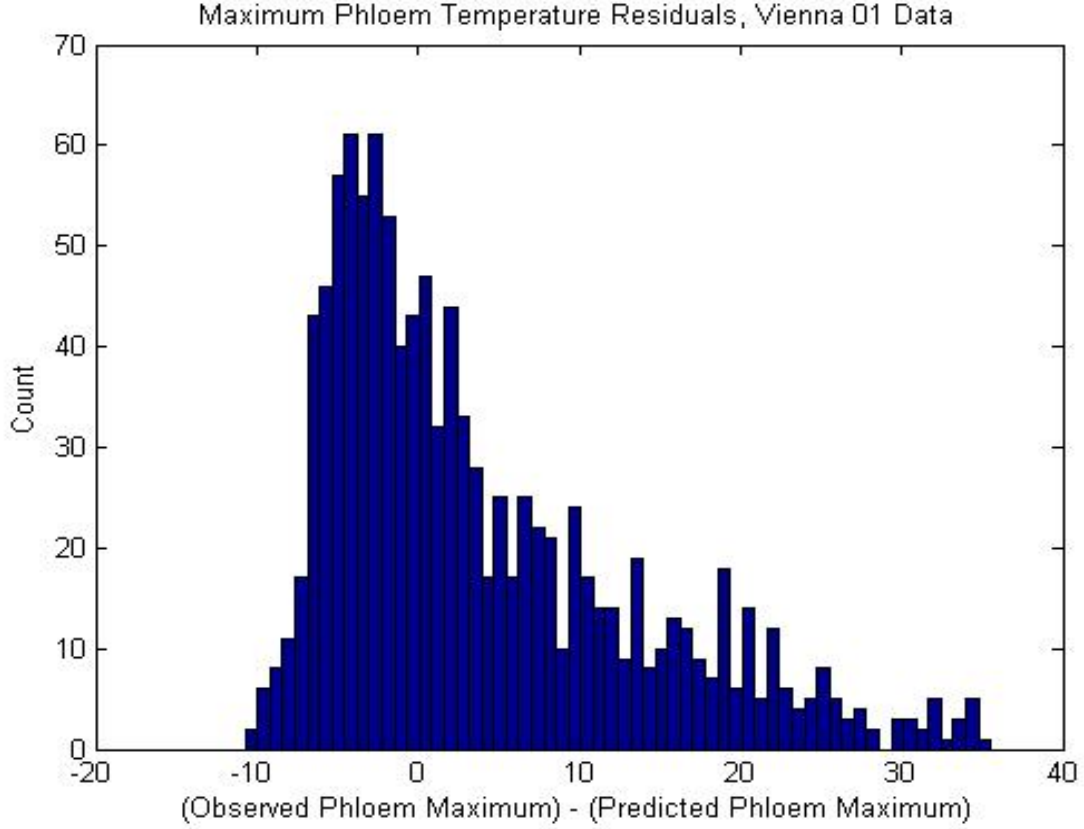


Figure 9: To account for the error in predicted maximum daily phloem temperatures on the southern bole aspect seen in figure 8, the difference between observed maximum daily phloem temperatures and predicted daily phloem temperatures was calculated (i.e.,  $\varepsilon = P_{max,obs} - P_{max,S}$ ) resulting in this histogram where predictions were generated from regression line found in figure 8(b) and the observed daily maximum southern bole aspect phloem temperatures of each tree observed at the Vienna site. When normalized to display relative frequencies, so the sum of all the boxes is 1, the histogram forms a probability density function (PDF) that describes the relative likelihood for the error,  $e$  to be a given amount. By calculating the cumulative sum of the normalized relative frequencies the corresponding cumulative distribution function (CDF) may be calculated (see figure 10) from which an hourly error adjustment can be calculated to better account for the observed variability seen in figure 8.

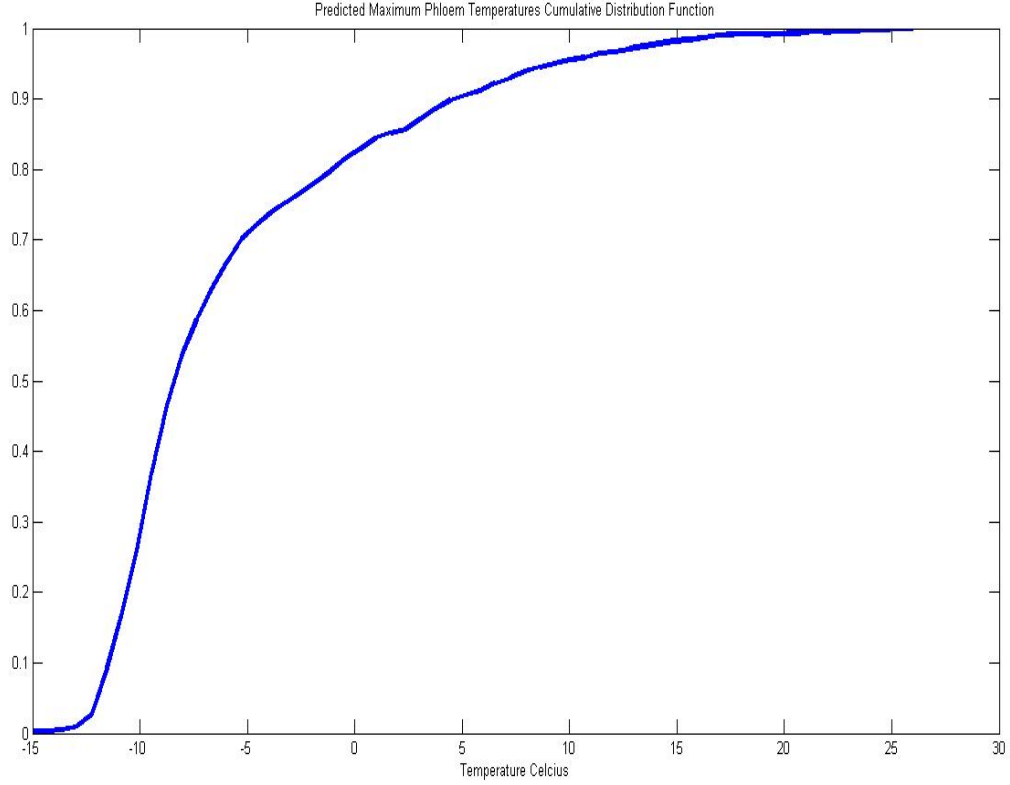


Figure 10: Scaled cumulative distribution function (CDF) used to estimate the error, attributed to solar insolation, between the predicted daily southern aspect phloem maximums (predictions are generated from regression line found in figure 8) and the observed daily maximum phloem temperatures at the Vienna site. Plot is the cumulative sum of the relative frequencies calculated from the probability density function (PDF) in figure 9. Now, let  $u \in [0, 1]$  and draw 365 random  $u$  values, one for each day of the year, from the Uniform(0,1) distribution. Call the CDF  $F(e)$  and set  $F(e) = u$  and compute  $F^{-1}(u)$  to get  $e$  values, which are draws from  $f(e)$ , the PDF described in figure 9, to estimate the observed error. Through this method of inverse-sampling the observed variability seen in figure 8 can be modeled from  $F(e)$ .

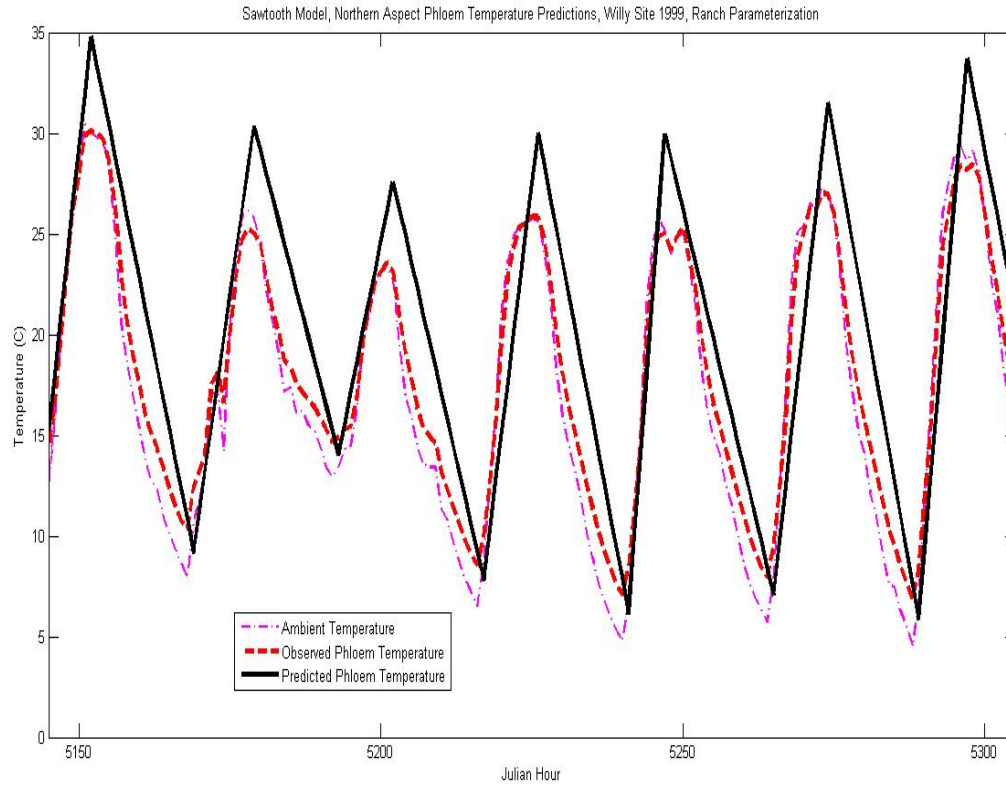


Figure 11: Plot of hourly northern bole aspect phloem temperature predictions generated by the Sawtooth model using the Ranch parameterization along with observed phloem and air temperatures from the Willy site in the SNRA. The Sawtooth model utilizes the daily phloem temperature maxima and minima models described in figures 5, 6, 7 and 8 to generate daily minimum and daily maximum phloem temperatures and, in sequence, linearly connects these daily extrema. The Sawtooth model is an attractive option since it is both elementary to understand and implement.



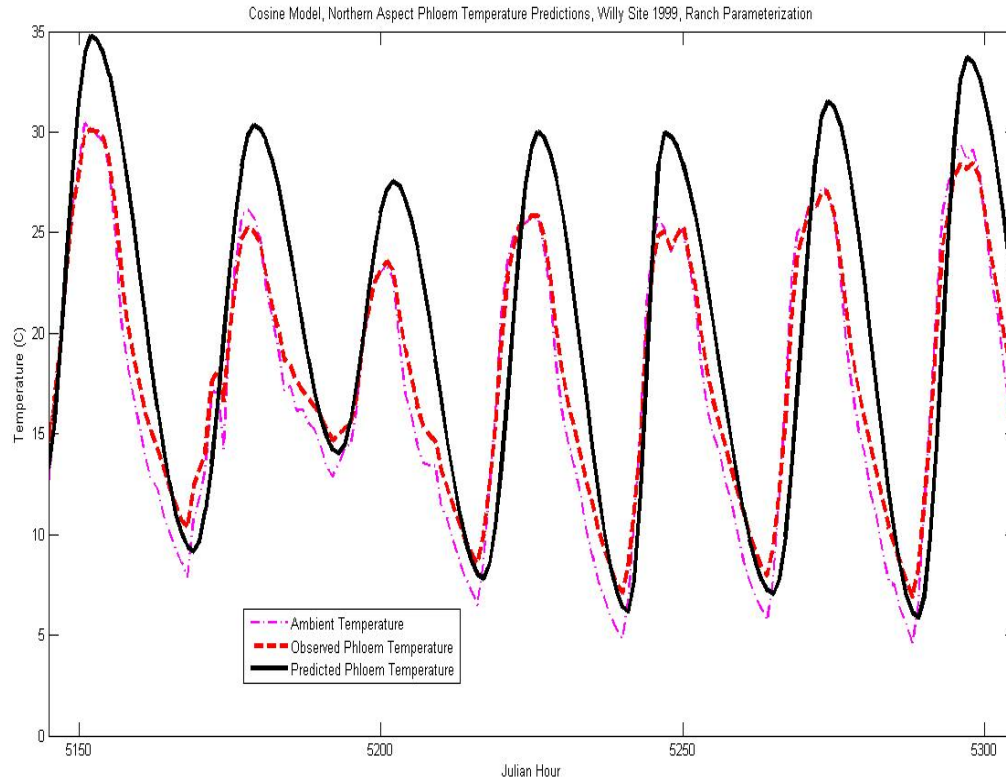


Figure 12: Plot of hourly northern bole aspect phloem temperature predictions generated by the Cosine model using the Ranch parameterization along with observed phloem and air temperatures from the Willy site in the SNRA. Like the Sawtooth model, the Cosine model utilizes the daily phloem temperature maxima and minima models described in figures 5, 6, 7 and 8 to generate daily minimum and daily maximum phloem temperatures and, in sequence, connects these daily extrema using a cosine wave. Similar to the Sawtooth model, the Cosine model is easy to implement and appears to exhibit curvature more similar to that seen in phloem temperature data.

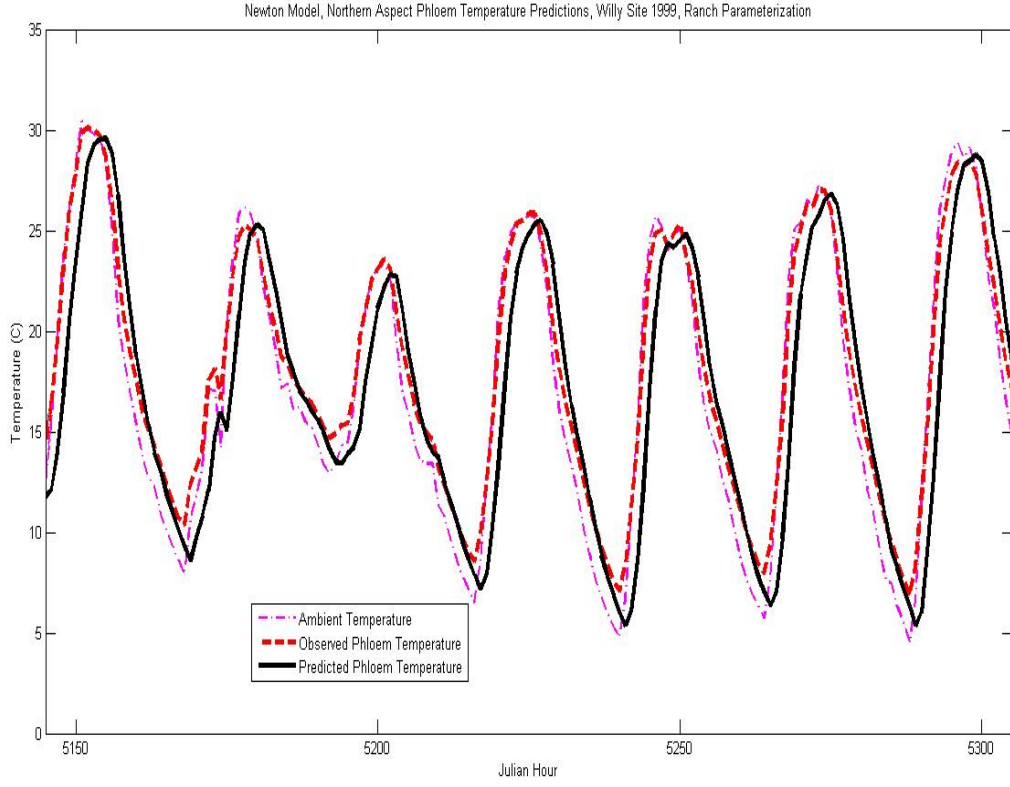


Figure 13: Plot of hourly northern bole aspect phloem temperature predictions generated by the Newton model using the Ranch parameterization along with observed phloem and air temperatures from the Willy site in the SNRA. The Newton model utilizes Newton's Law of Cooling, which states that the rate of change in phloem temperature is proportional to the difference between the current phloem temperature and the ambient temperature. We then have  $\frac{dP}{dt} = k(P - A)$  where  $A$  is the ambient temperature,  $P$  is the phloem temperature and  $k$ , the constant of proportionality, is the rate of temperature transfer. Upon discretizing, the Newton model takes the form  $P(t + \Delta t) = P(t) + k[P(t) - A(t)]\Delta t$ . The parameter  $k$  was estimated using linear regression and was found to be 0.5258 and 1.3357 under the Vienna and Ranch parameterizations respectively. As is seen in the figure, the Newton model closely predicts phloem temperatures on the northern bole aspect. However, whereas the previous models only required daily ambient maxima and minima, the Newton model requires hourly air temperatures.

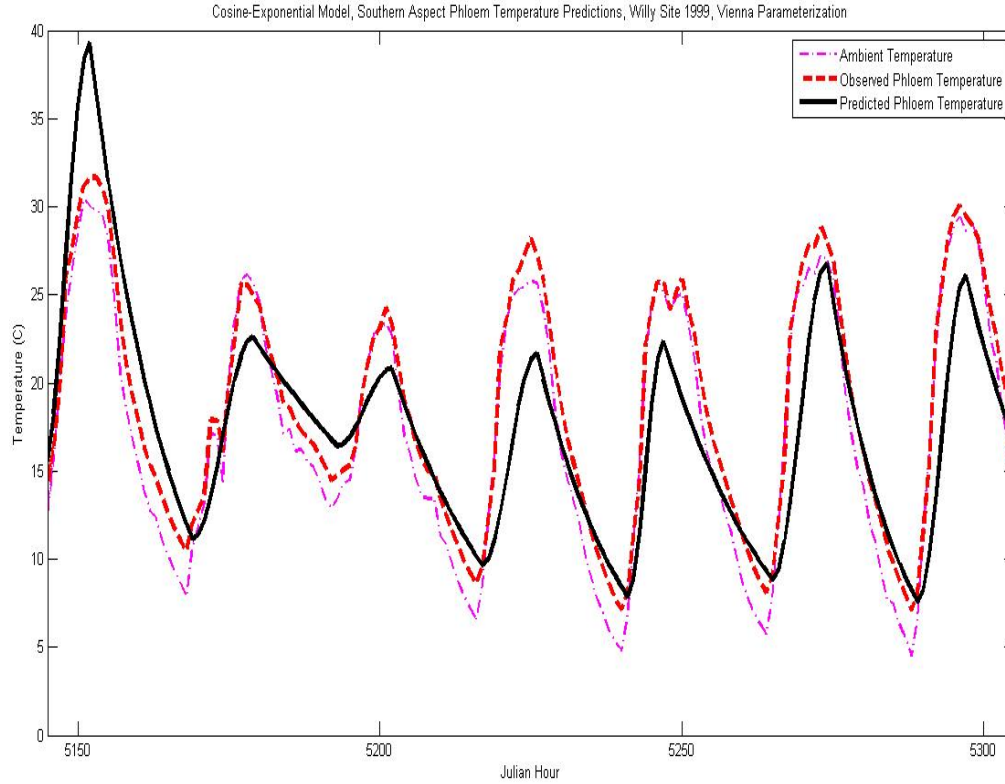


Figure 14: Plot of hourly southern bole aspect phloem temperature predictions produced by the Cosine-Exponential model using the Vienna parameterization. Also plotted are the observed southern bole aspect phloem temperatures as well as the corresponding ambient observations from the Willy site in the SNRA. As seen in figure 1, southern aspect phloem temperatures can differ greatly from both ambient and northern aspect phloem temperatures. The Cosine-Exponential model is designed to better match the shape of the southern aspect phloem temperatures. Similar to the Cosine and Sawtooth models, the Cosine-Exponential model sequentially connects the predicted daily phloem extrema produced from the phloem maxima and minima models described in figures 5, 6, 7 and 8. The Cosine-Exponential model uses a cosine wave to connect daily phloem minima predictions to daily phloem maxima predictions and an exponential curve to connect predicted phloem maxima to minima. Like the Sawtooth and Cosine model, the Cosine-Exponential model is an attractive option since it is both elementary in concept and implementation and only requires daily ambient extremes to function.

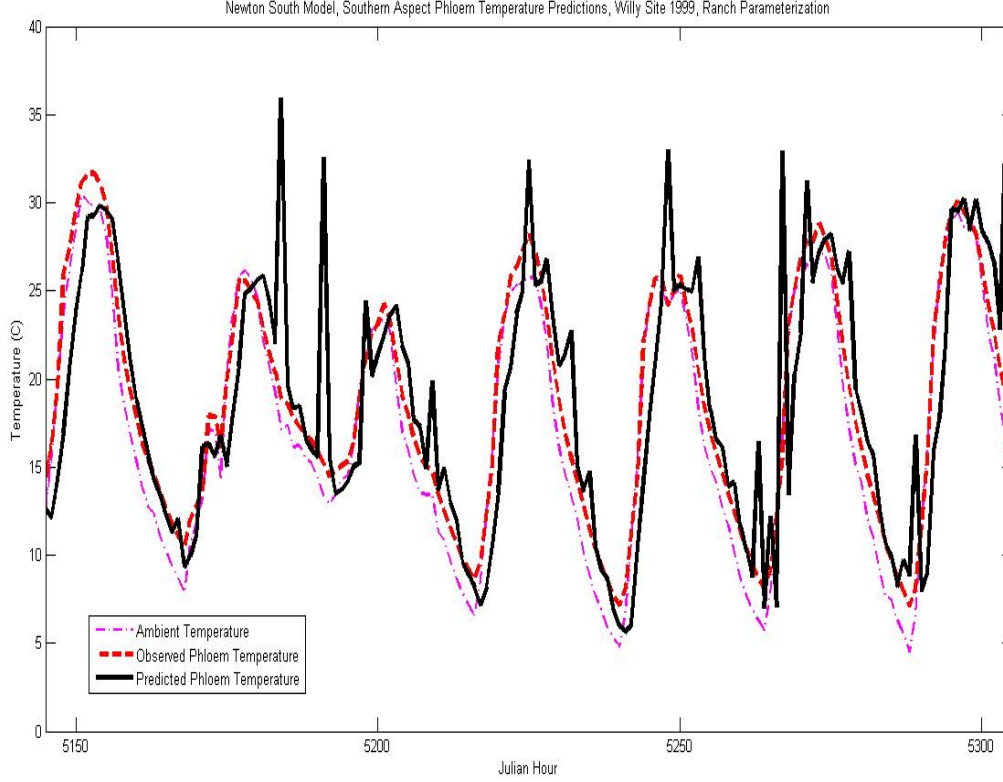


Figure 15: Plot of hourly southern bole aspect phloem temperature predictions produced by the Newton South model using the Ranch parameterization. Also plotted are the observed southern bole aspect phloem temperatures as well as the corresponding ambient observations from the Willy site in the SNRA. The Newton South model is an altered version of the Newton model used to produce southern bole aspect phloem temperatures since the original Newton model described in figure 13 does not perform well on the southern bole aspect. The Newton South model has the form  $\frac{dP}{dt} = k(P - A) + I$ , which, upon discretization, appears like this:  $P(t+1) = P(t) + k[P(t) - A(t)]\Delta t + I_t\Delta t$ . In the model,  $P$  represents phloem temperatures,  $A$  is ambient temperatures,  $k$  is the rate of temperature transfer (which was estimated in the Newton model) and the additional parameter,  $I$ , was added to the Newton model to account for the increased error outside Newton's Law of Cooling. To estimate the parameter  $I$ , residuals were used to generate a cumulative distribution function from which the hourly error parameter,  $I$ , was inverse-sampled. This is the same approach that was taken to adjust daily maximum phloem predictions on the southern aspect (figure 8). While the Newton South does not appear to match phloem temperatures, it does perform well. However, like the Newton model, the Newton South model requires hourly air temperatures in order to function.

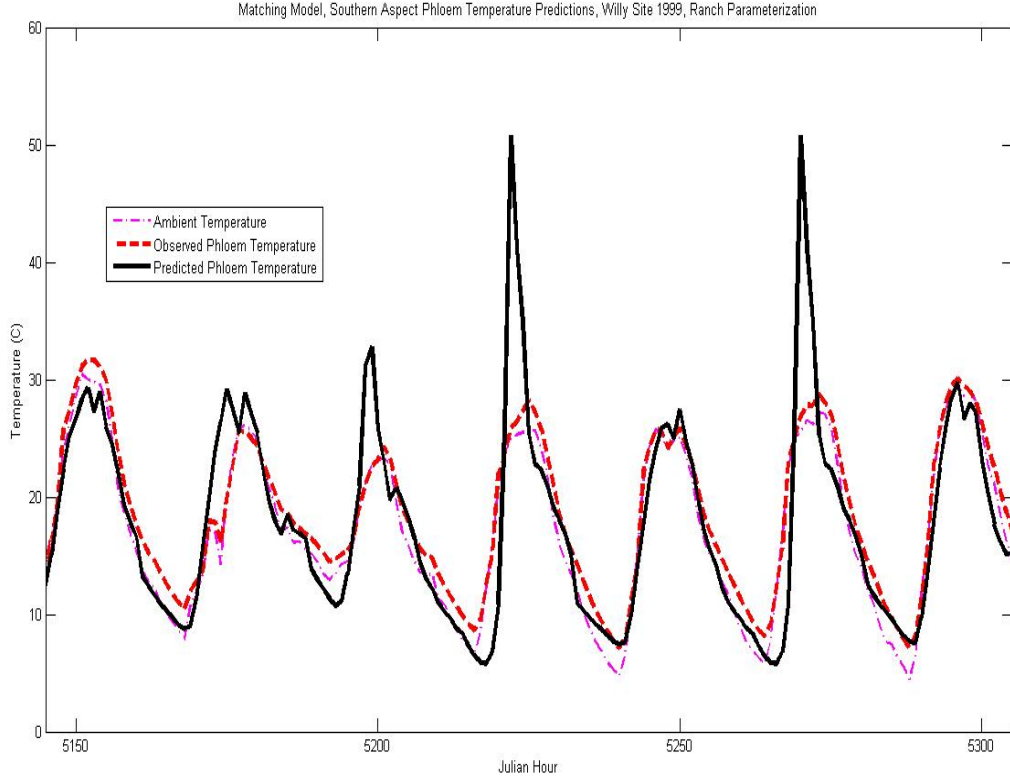


Figure 16: Plot of hourly southern bole aspect phloem temperature predictions generated by the Matching model using the Ranch parameterization along with observed phloem and air temperatures from the Willy site in the SNRA. To generate a prediction of hourly phloem temperatures for Julian day  $d$  that occurred under air temperature conditions where the minimum air temperature for day  $d$ ,  $A_{min}^d$ , the maximum air temperature for day  $d$ ,  $A_{max}^d$ , and the minimum air temperature for day  $d + 1$ ,  $A_{min}^{d+1}$ , are all known, the Matching model simply searches the archived set of daily ambient sequences of “*minimum, maximum, minimum*” for the closest match (based on sum of squares). It then returns the archive’s corresponding phloem temperatures as predicted phloem temperatures for Julian day  $d$ . In this case, the Ranch data is the archived data set discussed. The Matching model is a pragmatic approach to a complex question that utilizes existing knowledge to induce favorable results. Furthermore, the Matching model only requires daily ambient extrema in order to function.

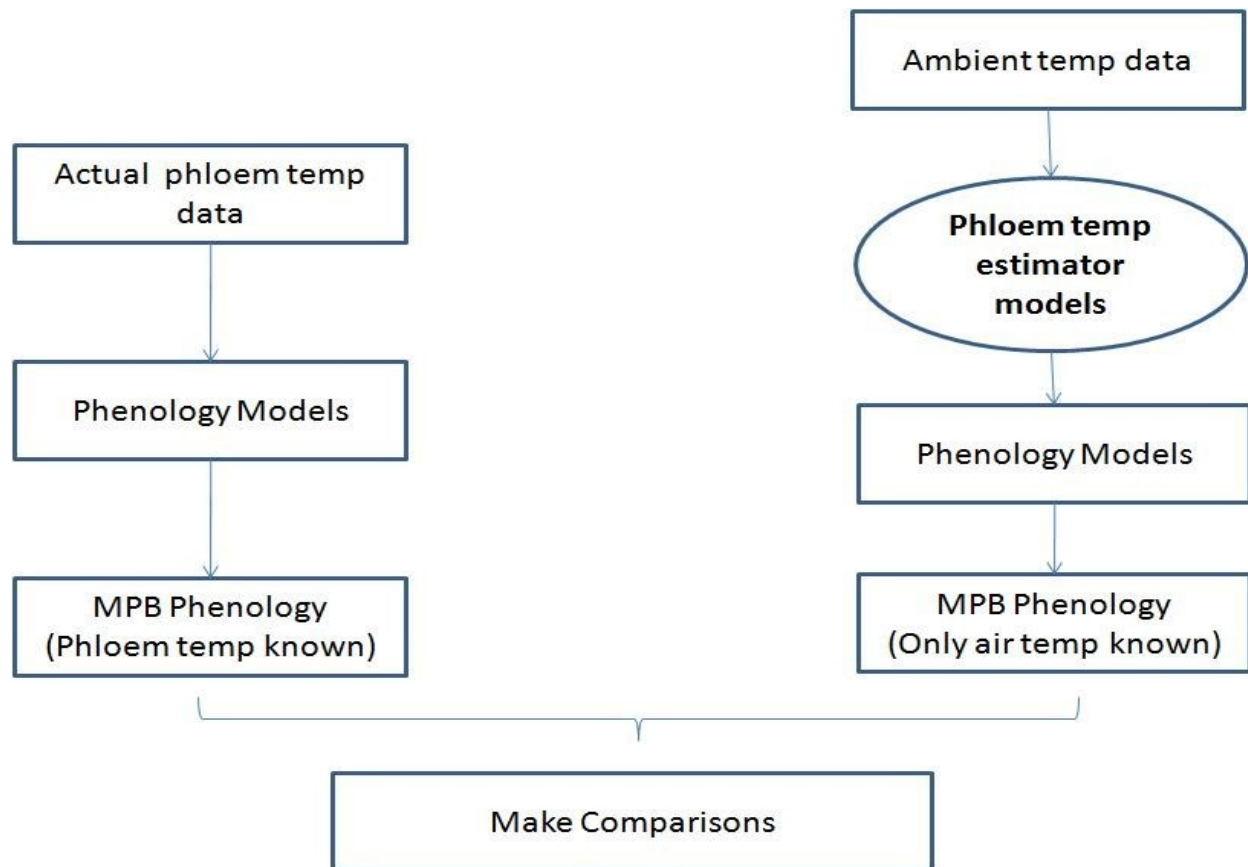


Figure 17: Flow-chart indicating how model performance is determined. On the left hand side, observed phloem temperatures are used as the argument in existing phenology models to generate a prediction regarding MPB phenology. On the right hand side, only air temperatures are known. Using the phloem temperature models discussed above, phloem temperatures are generated. The model-produced phloem temperatures are then inserted into the same phenology models as the observed temperatures were to yield another MPB phenology prediction. Note that phloem temperatures are not compared, rather, the results of the MPB phenology predictions are compared. By analyzing phenology results to determine model performance we emphasize the intent to generate phloem temperatures that maintain MPB phenology.

SNRA Results: Vienna Parameterization							
Northern Aspect Models		—Observed—	—Predicted—				
			Cosine	Newton	Sawtooth		
G-function: Cumulative  Error			290626	93560	232453		
Relative Error(Gfunct)			0.82	0.26	0.65		
R-function: $r^2$			0.03	0.44	0.50		
R-function: Average	1.29		1.51	1.08	1.76		
EvF: $r^2$			0.34	0.81	0.51		
Average 10%	193.36		178.00	195.00	185.10		
50%	198.25		182.60	200.30	189.00		
90%	203.73		186.50	205.70	192.80		
Volt: Percent Correct			36.36%	54.55%	36.36%		
Southern Aspect Models							
			Cosine	Cosine Exp.	Matching	Newton South	Sawtooth
G-function: Cumulative  Error			340183	188952	55639	42889	299728
Relative Error(Gfunct)			1.00	0.56	0.16	0.13	0.88
R-function: $r^2$			0.10	0.26	0.70	0.63	0.15
R-function: Average	1.92		0.04	0.84	1.65	1.96	0.23
EvF: $r^2$			0.04	0.05	0.59	0.91	0.07
Average 10%	185.36		140.10	157.20	182.30	184.50	157.10
50%	189.65		147.10	165.00	187.70	188.50	164.50
90%	193.75		153.90	173.00	192.90	193.10	171.60
Volt: Percent Correct			0.00%	9.09%	72.73%	72.73%	0.00%

Table 1: Results from the phenology models (G-function, R-function, Extended von Foerster, MPB Voltinism) driven by observed phloem temperatures compared to the results when driven by predicted phloem temperatures. Phloem temperature models were parameterized using data collected in 2001-2002 from the Vienna research site in the SNRA and observed phloem temperatures were collected in the SNRA from lodgepole pine. The G-function metric is simply the cumulative error between the curve(s) generated from observed phloem temperatures and the curve produced from predicted phloem temperatures over the seasonal oviposition window, JD 152 - JD 245. The relative G-function error is calculated to more easily assess model performance. With the R-function and the EvF metrics  $r^2$  values are calculated using MATLAB (Math Works 2010) as the primary metric while comparisons of the averaged growth rate, from the R-function, and the Julian date of the averaged emergence percentiles (from the EvF metric) indicate whether a poor performing model is over- or under-predicting developmental energy (i.e., if the predicted growth rate is less than the observed growth rate and the predicted emergence dates are later than observed emergence dates then the model likely under-predicts developmental energy). The MPB Voltinism metric calculates how often the predicted and observed voltinism results match. Observe that the Newton model performs best on the northern bole aspect while the Newton South and Matching models perform best on the southern bole aspect.

SNRA Results: Ranch Parameterization						
Northern Aspect Models	—Observed—	—Predicted—				
		Cosine	Newton	Sawtooth		
	G-function: Cumulative  Error	355215	75041	319540		
	Relative Error(Gfunct)	1.00	0.21	0.90		
	R-function: $r^2$	0.01	0.53	0.27		
	R-function: Average	1.29	1.48	1.23	2.09	
	EvF: $r^2$		0.21	0.81	0.44	
	Average 10%	193.36	176.90	192.20	182.20	
	50%	198.25	181.40	197.10	186.60	
	90%	203.73	185.40	202.30	190.20	
Volt: Percent Correct		27.27%	63.64%	27.27%		
Southern Aspect Models						
		Cosine	Cosine Exp.	Matching	Newton South	Sawtooth
G-function: Cumulative  Error		198490	289562	62885	46140	160504
Relative Error(Gfunct)		0.58	0.58	0.18	0.14	0.47
R-function: $r^2$		0.01	0.05	0.72	0.67	0.02
R-function: Average	1.92	1.20	0.24	1.80	1.85	1.17
EvF: $r^2$		0.48	0.20	0.80	0.84	0.35
Average 10%	185.36	195.20	196.00	189.20	185.50	200.50
50%	189.65	200.90	204.00	194.30	189.60	206.80
90%	193.75	206.70	212.90	199.20	193.70	212.80
Volt: Percent Correct		9.09%	9.09%	81.82%	81.82%	9.09%

Table 2: Results from the phenology models (G-function, R-function, Extended von Foerster, MPB Voltinism) driven by observed phloem temperatures compared to the results when driven by predicted phloem temperatures. Phloem temperature models were parameterized using data collected in 1996-1997 from the Ranch research site in the SNRA and observed phloem temperatures were collected in the SNRA from lodgepole pine. The G-function metric is simply the cumulative error between the curve(s) generated from observed phloem temperatures and the curve produced from predicted phloem temperatures over the seasonal oviposition window, JD 152 - JD 245. The relative G-function error is calculated to more easily assess model performance. With the R-function and the EvF metrics  $r^2$  values are calculated using MATLAB (Math Works 2010) as the primary metric while comparisons of the averaged growth rate, from the R-function, and the Julian date of the averaged emergence percentiles (from the EvF metric) indicate whether a poor performing model is over- or under-predicting developmental energy (i.e., if the predicted growth rate is less than the observed growth rate and the predicted emergence dates are later than observed emergence dates then the model likely under-predicts developmental energy). The MPB Voltinism metric calculates how often the predicted and observed voltinism results match. Observe that the Newton model performs best on the northern bole aspect while the Newton South and Matching models perform best on the southern bole aspect.



Northern Aspect SNRA MPB Voltinism: Vienna Parameterization				
Data Set	Observation(s)	Cosine	Newton	Sawtooth
Gold95	1	1/1	5/6	1/1
Gold96	4/5, 3/4, 2/3	1/1	10/13	1/1
Moose	2/3, 5/7	3/2	1/1	4/3
Ranch95	1	1/1	1/1	1/1
Ranch96	4/5, 12/17, 8/11	19/17	2/3	1/1
Smiley	1, 4/5	1/1	4/5	1/1
Vienna01	11/10, 1	5/4	1/1	15/13
Vienna03	1	4/3	1/1	11/9
Willy97	5/6, 9/11	1/1	3/4	1/1
Willy98	1	1/1	1/1	1/1
Willy99	1	11/9	1/1	10/9

Table 3: MPB Voltinism predictions generated in the SNRA from northern bole aspect observed and predicted phloem temperatures using the Vienna parameterization. Clearly, univoltine predictions from observed phloem temperatures are easier to match than the asynchronous fractional voltinism predictions. While the Newton model was closest, no model matched every univoltine prediction produced from observed phloem temperatures.

Northern Aspect SNRA MPB Voltinism: Ranch Parameterization				
Data Set	Observation(s)	Cosine	Newton	Sawtooth
Gold95	1	1/1	1/1	1/1
Gold96	4/5, 3/4, 2/3	8/7	1/1	1/1
Moose	2/3, 5/7	14/9	1/1	10/7
Ranch95	1	6/5	1/1	9/8
Ranch96	8/11, 12/17, 4/5	17/14	3/4	13/12
Smiley	1, 4/5	1/1	1/1	1/1
Vienna01	11/10, 1	4/3	1/1	5/4
Vienna03	1	11/8	1/1	4/3
Willy97	5/6, 9/11	1/1	11/14	1/1
Willy98	1	1/1	1/1	1/1
Willy99	1	6/5	1/1	10/9

Table 4: MPB Voltinism predictions generated in the SNRA from northern bole aspect observed and predicted phloem temperatures using the Ranch parameterization. While the univoltine predictions produced from observed phloem temperatures are easier to match than the asynchronous fractional voltinism predictions, only the Newton model matched each univoltine prediction produced from observed phloem temperatures.

Southern Aspect SNRA MPB Voltinism: Vienna Parameterization						
Data Set	Observation(s)	Cosine	Cosine Exp	Matching	Newton South	Sawtooth
Gold95	1	5/3	19/16	1/1	1/1	3/2
Gold96	1	8/5	1/1	1/1	1/1	10/7
Moose	1, 4/5	16/7	9/5	7/6	6/5	11/5
Ranch95	1	12/7	13/9	1/1	1/1	5/3
Ranch96	1	5/3	4/3	1/1	1/1	11/7
Smiley	1	13/9	12/11	1/1	1/1	7/6
Vienna01	11/10, 5/4, 11/9	12/7	4/3	11/10	14/13	7/4
Vienna03	10/9, 7/6	17/9	3/2	5/4	16/13	5/3
Willy97	1	7/4	4/3	1/1	1/1	20/13
Willy98	1	8/5	19/14	1/1	1/1	3/2
Willy99	1	15/8	13/10	19/16	1/1	7/4

Table 5: MPB Voltinism predictions generated in the SNRA southern bole aspect observed and predicted phloem temperatures using the Vienna parameterization. While the univoltine predictions produced from observed phloem temperatures are easier to match than the asynchronous fractional voltinism predictions, only the Newton South model, under the Vienna parameterization, matched every clearly univoltine prediction produced from observed phloem temperatures on the southern aspect. Now, the Matching model failed to produce a univoltine solution in only the Willy 99 case but was successful in matching the fractional voltinism produced from one of the Vienna 01 observed trees; the Newton South model prediction did not match in this case.

<b>Southern Aspect SNRA MPB Voltinism: Ranch Parameterization</b>						
Data Set	Observation(s)	Cosine	Cosine Exp	Matching	Newton South	Sawtooth
Gold95	1	5/7	2/3	1/1	1/1	2/3
Gold96	1	3/4	15/23	1/1	1/1	4/5
Moose	1, 4/5	10/11	1/1	1/1	8/7	1/1
Ranch95	1	5/6	10/13	1/1	1/1	5/6
Ranch96	1	5/7	3/4	1/1	1/1	3/4
Smiley	1	3/5	13/17	1/1	1/1	3/4
Vienna01	11/10, 5/4, 11/9	11/12	6/7	1/1	1/1	1/1
Vienna03	10/9, 7/6	1/1	1/1	12/11	7/6	1/1
Willy97	1	4/5	8/11	1/1	1/1	4/5
Willy98	1	3/4	13/20	1/1	1/1	3/4
Willy99	1	1/1	8/9	1/1	1/1	11/16

Table 6: MPB Voltinism predictions generated in the SNRA southern bole aspect observed and predicted phloem temperatures using the Ranch parameterization. While the univoltine predictions produced from observed phloem temperatures are easier to match than the asynchronous fractional voltinism predictions, both the Newton South and Matching model, under the Ranch parameterization, matched every clearly univoltine prediction produced from observed phloem temperatures on the southern aspect. Furthermore, the Newton South model was able to match the voltinism prediction generated from an observed tree in the Vienna 03 while the Matching model matched one in the Moose case.

RRR Results: Vienna Parameterization						
Northern Aspect Models	—Observed—	—Predicted—				
		Cosine	Newton	Sawtooth		
	G-function: Cumulative Error	295543.00	82028.00	257352.00		
	Relative Error(Gfunct)	0.91	0.25	0.79		
	R-function: $r^2$	0.54	NC	0.64		
	R-function: Average	0.13	0.89	0.72		
	EvF: $r^2$	0.52	0.97	0.45		
	Average 10%	288.13	226.88	303.25	210.75	
	50%	368.25	263.25	396.50	227.50	
	90%	501.38	372.50	517.88	251.63	
Volt: Percent Correct		0.00%	50.00%	0.00%		
Southern Aspect Models						
		Cosine	Cosine Exp.	Matching	Newton South	Sawtooth
G-function: Cumulative Error		444998.00	415194.00	208945.00	226087.00	433626.00
Relative Error(Gfunct)		1.00	0.93	0.47	0.51	0.97
R-function: $r^2$		0.04	0.18	0.91	0.87	0.10
R-function: Average	0.09	0.09	1.56	0.58	0.52	0.98
EvF: $r^2$		0.38	0.65	0.65	0.52	0.09
Average 10%	298.88	220.13	175.38	224.13	214.38	167.00
50%	390.63	234.63	182.88	249.25	229.38	174.63
90%	514.50	252.13	189.00	294.38	261.75	181.75
Volt: Percent Correct		0.00%	0.00%	0.00%	0.00%	0.00%

Table 7: Results from the phenology models (G-function, R-function, Extended von Foerster, MPB Voltinism) driven by observed phloem temperatures compared to the results when driven by predicted phloem temperatures. Phloem temperature models were parameterized using data collected in 2001-2002 from the Vienna research site in the SNRA and observed phloem temperatures were collected at the Railroad Ridge site from high-elevation whitebark pine. The G-function metric is simply the cumulative error between the curve(s) generated from observed phloem temperatures and the curve produced from predicted phloem temperatures over the seasonal oviposition window, JD 152 - JD 245. The relative G-function error is calculated to more easily assess model performance. With the R-function and the EvF metrics  $r^2$  values are calculated using MATLAB (Math Works 2010) as the primary metric while comparisons of the averaged growth rate, from the R-function, and the Julian date of the averaged emergence percentiles (from the EvF metric) indicate whether a poor performing model is over- or under-predicting developmental energy (i.e., if the predicted growth rate is less than the observed growth rate and the predicted emergence dates are later than observed emergence dates then the model likely under-predicts developmental energy). The MPB Voltinism metric calculates how often the predicted and observed voltinism results match. At the RRR site, each voltinism prediction generated from observed temperatures was fractional and thus, difficult to match (see figure 4). Hence, it is remarkable that the Newton model matched voltinism predictions 50% of the time on the northern bole aspect. NC stands for not computable since the Newton model always induced a zero growth rate. This result exactly matches the growth rate produced by observed phloem temperatures in all but one year and is thus the best result under the R-function metric. Observe that the Newton model performs best on the northern bole aspect while the Matching model performs best on the southern bole aspect.

RRR Results: Ranch Parameterization						
Northern Aspect Models	—Observed—		—Predicted—			
			Cosine	Newton	Sawtooth	
	G-function: Cumulative Error		324438.00	48669.00	304443.00	
	Relative Error(Gfunct)		1.00	0.15	0.94	
	R-function: $r^2$		0.48	NC	0.50	
	R-function: Average	0.13	1.50	0.00	1.38	
	EvF: $r^2$		0.72	0.98	0.35	
	Average 10%	288.13	199.38	292.00	204.00	
	50%	368.25	204.38	378.75	209.88	
	90%	501.38	209.50	503.25	243.13	
Volt: Percent Correct		0.00%	62.50%	0.00%		
Southern Aspect Models						
		Cosine	Cosine Exp.	Matching	Newton South	Sawtooth
G-function: Cumulative Error		161727.00	216965.00	93522.00	183600.00	148218.00
Relative Error(Gfunct)		0.36	0.49	0.21	0.41	0.33
R-function: $r^2$		NC	1.00	NC	1.00	0.06
R-function: Average	0.09	0.00	0.17	0.00	0.29	0.11
EvF: $r^2$		0.31	0.50	0.80	0.62	0.66
Average 10%	298.88	221.25	211.13	252.13	222.13	230.25
50%	390.63	240.13	222.13	338.50	248.88	263.50
90%	514.50	305.13	246.25	475.88	296.50	373.63
Volt: Percent Correct		0.00%	0.00%	25.00%	0.00%	12.50%

Table 8: Results from the phenology models (G-function, R-function, Extended von Foerster, MPB Voltinism) driven by observed phloem temperatures compared to the results when driven by predicted phloem temperatures. Phloem temperature models were parameterized using data collected in 1996-1997 from the Ranch research site in the SNRA and observed phloem temperatures were collected at the Railroad Ridge site from high-elevation whitebark pine. The G-function metric is simply the cumulative error between the curve(s) generated from observed phloem temperatures and the curve produced from predicted phloem temperatures over the seasonal oviposition window, JD 152 - JD 245. The relative G-function error is calculated to more easily assess model performance. With the R-function and the EvF metrics  $r^2$  values are calculated using MATLAB (Math Works 2010) as the primary metric while comparisons of the averaged growth rate, from the R-function, and the Julian date of the averaged emergence percentiles (from the EvF metric) indicate whether a poor performing model is over- or under-predicting developmental energy (i.e., if the predicted growth rate is less than the observed growth rate and the predicted emergence dates are later than observed emergence dates then the model likely under-predicts developmental energy). The MPB Voltinism metric calculates how often the predicted and observed voltinism results match. At the RRR site, each voltinism prediction generated from observed temperatures was fractional and thus, difficult to match (see figure 4). Hence, it is remarkable that the Newton model matched voltinism predictions 62.5% of the time on the northern bole aspect and the Matching model matched voltinism predictions 25% of the time on the southern bole aspect. NC stands for not computable since the Newton model always induced a zero growth rate. This result exactly matches the growth rate produced by observed phloem temperatures in all but one year. The  $r^2$  values of 1.00 under the Cosine-Exponential and Newton South models are due to rounding error. The actual values are less than one and thus, the growth rate produced using these models did not match the rate produced from observed phloem temperatures at least twice. Hence, NC is again the best result under the R-function metric as 0.00 is the exact growth rate produced by the observed phloem temperatures in all but one instance. Again, note that the Newton model performs best on the northern bole aspect while the Matching model performs best on the southern bole aspect.

Dixie Results: Vienna Parameterization							
Northern Aspect Models		—Observed—		—Predicted—			
			Cosine	Newton	Sawtooth		
G-function: Cumulative Error			22573.00	29143.00	22331.00		
Relative Error(Gfunct)			0.64	0.83	0.63		
R-function: $r^2$			N/A	N/A	N/A		
R-function: Average	3.66		3.13	2.13	3.33		
EvF: $r^2$			0.98	1.00	0.98		
Average 10%	197.50		186.00	201.00	190.00		
50%	200.75		189.00	204.00	193.00		
90%	203.5		193.00	207.00	197.00		
Volt: Percent Correct			0.00%	100.00%	0.00%		
Southern Aspect Models			Cosine	Cosine Exp.	Matching	Newton South	Sawtooth
G-function: Cumulative Error			46790.00	44526.00	9102.00	7754.00	44586.00
Relative Error(Gfunct)			1.00	0.95	0.19	0.17	0.95
R-function: $r^2$			N/A	N/A	N/A	N/A	N/A
R-function: Average	3.65		0.00	0.00	3.32	3.13	0.00
EvF: $r^2$			0.99	0.99	0.99	0.96	1.00
Average 10%	195.00		138.00	152.00	190.00	190.00	140.00
50%	198.75		147.00	159.00	194.00	193.00	153.00
90%	201.25		155.00	166.00	198.00	197.00	161.00
Volt: Percent Correct			0.00%	0.00%	100.00%	100.00%	0.00%

Table 9: Results from the phenology models (G-function, R-function, Extended von Foerster, MPB Voltinism) driven by observed phloem temperatures compared to the results when driven by predicted phloem temperatures. Phloem temperature models were parameterized using data collected in 2001-2002 from the Vienna research site in the SNRA and observed phloem temperatures were collected in the DNF from ponderosa pine. The G-function metric is simply the cumulative error between the curve(s) generated from observed phloem temperatures and the curve produced from predicted phloem temperatures over the seasonal oviposition window, JD 152 - JD 245. The relative G-function error is calculated to more easily assess model performance. In this case, there is only one observation year for this site so  $r^2$  values are not applicable in the R-function metric. Instead, simple comparison of growth rates indicate model performance under the R-function metric. For the EvF metric  $r^2$  values are calculated using MATLAB (Math Works 2010) as the primary metric while comparisons of the averaged growth rate, from the R-function, and the Julian date of the averaged emergence percentiles (from the EvF metric) indicate whether a poor performing model is over- or under-predicting developmental energy (i.e., if the predicted growth rate is less than the observed growth rate and the predicted emergence dates are later than observed emergence dates then the model likely under-predicts developmental energy). The MPB Voltinism metric calculates how often the predicted and observed voltinism results match. In this case, each tree observed generated a univoltine prediction. This was matched on the northern bole aspect by the Newton model and on southern bole aspect by the Newton South and Matching models. Observe that the Newton model performs best on the northern bole aspect while the Matching model performs best on the southern bole aspect.

Dixie Results: Ranch Parameterization							
Northern Aspect Models		—Observed—		—Predicted—			
			Cosine	Newton	Sawtooth		
G-function: Cumulative Error			35187.00	27243.00	34805.00		
Relative Error(Gfunct)			1.00	0.77	0.99		
R-function: $r^2$			N\A	N\A	N\A		
R-function: Average	3.66		3.18	2.17	3.53		
EvF: $r^2$			1.00	1.00	1.00		
Average 10%	197.50		183.00	199.00	187.00		
50%	200.75		187.00	203.00	190.00		
90%	203.50		190.00	206.00	193.00		
Volt: Percent Correct			0.00%	100.00%	0.00%		
Southern Aspect Models							
			Cosine	Cosine Exp.	Matching	Newton	Sawtooth
G-function: Cumulative Error			22260.00	37342.00	24726.00	6308.00	22378.00
Relative Error(Gfunct)			0.48	0.80	0.53	0.13	0.48
R-function: $r^2$			N/A	N/A	N/A	N/A	N/A
R-function: Average	3.65		2.32	2.24	2.78	3.14	2.19
EvF: $r^2$			1.00	0.97	1.00	1.00	0.96
Average 10%	195.00		190.00	190.00	196.00	192.00	202.00
50%	198.75		198.00	195.00	201.00	196.00	205.00
90%	201.25		203.00	201.00	204.00	199.00	209.00
Volt: Percent Correct			100.00%	100.00%	100.00%	100.00%	100.00%

Table 10: Results from the phenology models (G-function, R-function, Extended von Foerster, MPB Voltinism) driven by observed phloem temperatures compared to the results when driven by predicted phloem temperatures. Phloem temperature models were parameterized using data collected in 1996-1997 from the Ranch research site in the SNRA and observed phloem temperatures were collect in the DNF from ponderosa pine. The G-function metric is simply the cumulative error between the curve(s) generated from observed phloem temperatures and the curve produced from predicted phloem temperatures over the seasonal oviposition window, JD 152 - JD 245. The relative G-function error is calculated to more easily assess model performance. In this case, there is only one observation year for this site so  $r^2$  values are not applicable in the R-function metric. Instead, simple comparison of growth rates indicate model performance under the R-function metric. For the EvF metric  $r^2$  values are calculated using MATLAB (Math Works 2010) as the primary metric while comparisons of the averaged growth rate, from the R-function, and the Julian date of the averaged emergence percentiles (from the EvF metric) indicate whether a poor performing model is over- or under-predicting developmental energy (i.e., if the predicted growth rate is less than the observed growth rate and the predicted emergence dates are later than observed emergence dates then the model likely under-predicts developmental energy). The MPB Voltinism metric calculates how often the predicted and observed voltinism results match. In this case, each tree observed generated a univoltine prediction. This was matched on the northern bole aspect by the Newton model and on southern bole aspect by every model. Observe that the Newton model performs best on the northern bole aspect while the Matching model perform best on the southern bole aspect.

## References

- G.D. Amman. Characteristics of mountain pine beetles reared in four pine hosts. *Environmental Entomology*, 1982.
- G.D. Amman and R.F. Schmitz. Mountain pine beetle - lodgepole pine interactions and strategies for reducing tree losses. *Ambio*, 1988.
- M.P. Ayres and M.J. Lombardero. Assessing the consequences of global change for forest disturbance from herbivores and pathogens. *The Science of the Total Environment*, 2000.
- B. Bentz, J. Régnière, C. Fettig, E. Hansen, J. Hayes, J. Hicke, R. Kelsey, J. Negrón, and S. Seybold. Climate change and bark beetles of the western united states and canada: Direct and indirect effects. *BioScience*, 2010.
- B.J. Bentz and D.E. Mullins. Ecology of mountain pine beetle (coleoptera: Scolytidae) cold hardening in the intermountain west. *Environmental Entomology*, 1999.
- P.V. Bolstad, B.J. Bentz, and J.A. Logan. Modelling micro-habitat temperature for dendroctonus ponderosae (coleoptra: scolytidae). *Ecological Modelling*, 1997.
- A.L. Carroll, S.W. Taylor, J. Régnière, and L. Safranyik. Effects of climate change on range expansion by the mountain pine beetle in british columbia. in: Shore t.l., j.e. brooks, j.e. stone, (editors). mountain pine beetle symposium: Challenges and solutions. canadian forest service, victoria bc. inf. rep. bc-x-399. 2004.
- E. Gilbert, J.A. Powell, J.A. Logan, and B.J. Bentz. Comparison of three models predicting developmental milestones given environmental and individual variation. *Bulletin of Mathematical Biology*, 2004.
- J.A. Hicke, J.A. Logan, J.A. Powell, and D.S. Ojima. Changing temperatures influence suitability for modeled mountain pine beetle (dendroctonus ponderosae) outbreaks in the western united states. *J. Geophys. Res*, 2006.
- J.L. Jenkins, J.A. Powell, J.A. Logan, and B.J. Bentz. Low seasonal temperatures promote life cycle synchronization. *Bulletin of Mathematical Biology*, 2001.



- J.A. Logan and B.J. Bentz. Model analysis of mountain pine beetle (coleoptera: Scolytidae) seasonality. *Environmental-Entomology*, 1999.
- J.A. Logan and J.A. Powell. Ghost forests, global warming, and the mountain pine beetle (coleoptera: Scolytidae). *American Entomologist*, 2001.
- J.A. Logan, J. Régnière, and J.A. Powell. Assessing the impacts of global warming on forest pest dynamics. *Frontiers in Ecology and the Environment*, 2003.
- D.J. Mattson and C. Jonkel. Stone pines and bears. *General Technical Report - US Department of Agriculture, Forest Service*, 1990.
- M.D. McGregor and D.M. Cole. Integrating management strategies for the mountain pine beetle with multiple-resource management of lodgepole pine forest. *US Dep. Agric., For. Serv., Interm. For, and Range Exp. Stn. Gen. Tech. Rpt. INT-17*, 1985.
- A.G. McKendrick. The application of mathematics to medical problems. *Proc. Edinb. Math. Soc.*, 1926.
- R. Means. Synthesis for lower treeline limber pine (*pinus flexilis*) woodland knowledge, research needs, and management considerations. *USDA Forest Service Proceedings RMRS-P-63*, 2011.
- J.A. Powell and B.J. Bentz. Connecting phenological predictions with population growth rates for mountain pine beetle, an outbreak insect. *Landscape Ecology*, 2009.
- J.A. Powell and J.A. Logan. Insect seasonality: circle map analysis of temperature-driven life cycles. *Theoretical Population Biology*, 2005.
- L. Safranyik, D.M. Shrimpton, and H.S. Whitney. Management of lodgepole pine to reduce losses from the mountain pine beetle. *Forestry Technical Report 1, Department of the Environment, Pacific Forest Research Centre, Victoria, BC.*, 1974.
- K. Trán, T. Ylioja, R.F. Billings, Rénière, and M.P. Ayres. Impact of minimum winter temperatures on the population dynamics of *dendroctonus frontalis*. *Ecological Applications*, 2007.
- W.J. Volney and K.G. Hirsch. Disturbing forest disturbances. *The Forestry Chronicle*, 2005.

H. von Foerster. Some remarks on changing populations. *The Kinetics of Cellular Proliferation*, 1959.

Math Works. Matlab reference guide. *Natick MA*, 2010.